



Exploring the influence of fertilization on bacterial community fluctuations in *Ulva* cultivation

Paul Estoup^{a,b,*}, Vincent Gernigon^c, Amandine Avouac^b, Guillaume Blanc^{a,*}, Angélique Gobet^{b,**}

^a MIO, Aix Marseille Université, Université de Toulon, CNRS, IRD, UM 110, Marseille, France

^b MARBEC, Univ Montpellier, CNRS, Ifremer, IRD, Sète, France

^c Eranova, Port-Saint-Louis-du-Rhône, France

ARTICLE INFO

Keywords:

Algal aquaculture
Ulva holobiont
 Macroalgae-bacteria interactions
 Seaweed holobiont

ABSTRACT

Ulva are green algae known for their biomass accumulation on the coast due to eutrophication. As these algae are able to bioremediate nitrate loadings, they are used as biofilters of enriched waters in aquaculture. *Ulva* form a holobiont by naturally hosting various microbes, also involved in nitrate metabolism. However, little is known about fluctuations of the *Ulva* holobiont in fertilized waters over time. We surveyed fluctuations of the bacterial community associated with *Ulva lacinulata* cultivation, with (enriched, ENR) and without (seawater only, SW) nitrate-based fertilization. *Ulva* biofilm and cultivation water were regularly collected and contextual parameters (nutrients, temperature, pH) were regularly measured over twelve weeks. Metabarcoding of the 16S rDNA in the biofilm and water compartments revealed that fertilization led to higher alpha-diversity. Diversity patterns indicated that samples clustered together for each compartment in SW or ENR. Fertilization led to a different genus composition in the water after 5 days, and it led to a more even community in the biofilm, from few very dominant genera at the beginning of the experiment to more less dominant genera at the end. The core microbiota in the biofilm common to SW and ENR was mainly composed of genera involved in the host fitness and physiology. Core genera common to SW and ENR in the water were likely benefiting from the culture conditions. Microbiota's predicted metabolic pathways revealed a heightened capacity for nitrate reduction in ENR. These results may serve as a foundation to understand nitrate loadings impact on *Ulva*'s microbiota in eutrophication conditions.

1. Introduction

Green algae from the genus *Ulva* are mostly known for their biomass accumulation on the coastline of industrialized countries as a consequence of increasing anthropogenic activities combined with climate change (e.g. factory livestock, agriculture) [1–5]. This common phenomenon has been seen worldwide such as on the coasts of the Yellow Sea, the English Channel, or Mediterranean lagoons [6–9] and it is enhanced by high nutrient availability when physical conditions are favorable [10]. Coastal blooms of *Ulva* sp. have been mostly associated

with high nitrogen loadings, from atmospheric or wastewater origin, fertilizer use, and include organic nitrogen, ammonium and nitrate in particular [3,8,11]. Decomposing beached *Ulva* sp. lead to the production of harmful gases such as CO₂ and H₂S, and this is mainly due to the metabolic activity of associated bacteria [2,12,13].

Marine macroalgae are colonized by various organisms, including other macroalgae (e.g. the genus *Myrionema strangulans* on *Ulva* sp. Thalli) [14,15] and microorganisms (e.g. procaryotes, protists, fungi, virus), forming the macroalgal holobiont altogether [14,16]. The macroalgal surface hosts high-densities of microorganisms with about 10² to

Abbreviations: ENR, Nitrate-based fertilization; SW, Sea-Water only; IMTA, Integrated Multi-Trophic Aquaculture; HRAP, High-Rate Algal Ponds; ASV, Amplicon sequence variant; OTU, Operational Taxonomic Unit; SRRA, Sample's Reaction Relative Abundance; PBI, Prevalence Bias Index; DNRA, Dissimilatory Reduction of Nitrate to Ammonium; ANRA, Assimilatory Nitrate Reduction to Ammonium.

* Correspondence to P. Estoup and G. Blanc, MIO, Aix Marseille Université, Université de Toulon, CNRS, IRD, UM 110, Campus de Luminy case 901, 163 Av. de Luminy, 13288 Marseille cedex 9, France.

** Correspondence to A. Gobet, MARBEC, Univ Montpellier, CNRS, Ifremer, IRD, Avenue Jean Monnet CS 30171, 34203 Sète cedex, France.

E-mail addresses: paul.ESTOUP@univ-amu.fr (P. Estoup), guillaume.blanc@mio.osupytheas.fr (G. Blanc), angelique.gobet@ifremer.fr (A. Gobet).

<https://doi.org/10.1016/j.algal.2024.103688>

Received 20 April 2024; Received in revised form 20 August 2024; Accepted 28 August 2024

Available online 31 August 2024

2211-9264/© 2024 The Authors. Published by Elsevier B.V. This is an open access article under the CC BY license (<http://creativecommons.org/licenses/by/4.0/>).

10^7 cells per cm^2 , depending on the macroalgal species, the season and the morphological part of the alga [17,18]. In the macroalgal holobiont, microorganisms interact with the algal host and, while having an effect on its physiology (e.g. nutrient supply, host defense, host development) [16,19–21], the host also “gardens” its epiphytic microbial community by attracting and maintaining species of interest for its health (i.e. the microbial gardening concept) [22,23]. As an example, *Ulva mutabilis* gardens its microbiota in cultivation conditions by producing dimethylsulfoniopropionate (DMSP), an osmolyte attracting the bacterium *Roseovarius* sp. MS2 [24]. Varying environmental conditions such as nutrient concentration, temperature, pH, also directly impact the macroalgal holobiont. It modifies the host health and physiology, the microbial community composition and distribution, and the interactions between the host and its associated microbiota (e.g. dysbiosis state of the microbiota leading to a diseased host) [25,26]. The importance of *Ulva*'s microbiota on the host development has been shown since early on [20,27]. Indeed, some *Ulva* species are known to harbor a bacterial community with members producing indispensable signaling molecules for the morphological development of the thallus [28,29]. For instance, *Roseovarius* sp. and *Maribacter* sp. produce regulatory factors inducing a similar action as the plant hormones cytokinin and auxin in the development and morphogenesis of *Ulva mutabilis* and *Ulva intestinalis*. These factors were identified as growth and morphogenesis-promoting (AGMPFs) such as thallusin [30,31]. Additionally, *Ulva mutabilis* cultivated together with high concentrations of the strains of the genera *Roseovarius* and *Maribacter*, is resistant to micropollutants such as antibiotic and herbicides and even has the ability to remove endocrine disruptors from the environment [32].

As a solution to bioremediate wastewater with high nitrogen loadings, *Ulva* may be used as a biofilter, as in integrated multitrophic aquaculture (IMTA) for instance [33,34]. Some IMTA systems consist in using mariculture fishpond effluents, generally containing high concentrations of ammonia, nitrate and phosphate as well as an associated microbial community, to fertilize algae such as *Ulva*. These culture conditions have been shown to provide algal growth- and morphogenesis-promoting factors to *Ulva* and to contain known morphogenesis-inducing bacteria [31]. To our knowledge, still few studies have investigated bacterial communities associated with *Ulva* cultures and the nutrient composition in the cultivation water was not always determined. For instance, *Ulva fasciata* cultivation in fish-pond effluents in an IMTA system at the Gulf of Aqaba (Eilat, Israel) has also shown taxonomic composition fluctuations in spring over 5 weeks [35]. However, fluctuations of the bacterial community composition linked to other culture conditions or nutrient content have not been surveyed to our knowledge.

Here, we hypothesized that the artificial addition of nutrients in *Ulva* cultures has an effect on the bacterial community composition at the *Ulva*'s surface and in the cultivation water. Thalli of *Ulva* were cultivated in natural seawater in raceways over twelve weeks with or without addition of a nitrate-based fertilizer. The bacterial community from the cultivated water and from the *Ulva* microbial surface (hereafter referred to as the *Ulva* biofilm) was regularly sampled and surveyed using a metabarcoding approach and contextual parameters (nutrients, pH, temperature) were measured in parallel. This sampling design aimed at tackling the following questions: (i) Does the use of a nitrate-based fertilizer influence the bacterial community composition and succession associated with *Ulva* cultivation? (ii) Does the use of such fertilizer influence similarly the cultivation water and the *Ulva* biofilm? (iii) Is there an impact of the nitrate-based fertilizer on the potential bacterial community functioning?

2. Materials and methods

2.1. Experimental strategy

Ulva were cultivated in two High Rate Algal Ponds (HRAP) [36] of

160 m^3 with water mixing maintained at $0.2 \text{ m}\cdot\text{s}^{-1}$ by a Coldep® vacuum airlift column [37]. Cultures were done at the marine experimental platform from the French National Institute for Ocean Science (Institut Français de Recherche pour l'Exploitation de la Mer, IFREMER) at Palavas-les-Flots, France by the industrial partner ERANOVA (they upcycle *Ulva* for bio-based, recyclable, compostable resins, see more here: <https://eranovabioplastics.com/?lang=en>). The two HRAP were filled in with coastal seawater filtered at $100 \mu\text{m}$ and with the same inoculum of *Ulva* thalli collected from the adjacent Prévost lagoon (43.52°N , 3.9°E). To ensure uniform mixing in the HRAP, *Ulva* specimens were manually stirred daily from Monday to Friday between 8 and 10 am, using a rake. Two culture conditions were processed simultaneously with (i) an enrichment of a nitrate-based fertilizer (culture medium: $0.217 \text{ g}\cdot\text{L}^{-1}$ of KNO_3 at 100% of purity, $0.004 \text{ g}\cdot\text{L}^{-1}$ of P_2O_5 at 84% and $0.5 \text{ g}\cdot\text{L}^{-1}$ of NaOH at 97%; hereafter referred as enriched, ENR), and (ii) without enrichment with only seawater (seawater only, SW). ENR cultivation was conducted in a batch mode, consisting in a monthly water renewal together with fertilizer supplementation. Batches were programmed by the industrial partner, ERANOVA, independently of our study. A total of 4 batches were done: March 3rd–April 1st (including days D0–D26), April 2nd–18th (D29–D41), April 19th–May 2nd (D46–D54), and May 3rd–25th 2021 (D60–D82). No fertilizer was added in the 3rd batch (D46–D54). SW cultivation consisted in fresh filtered seawater continuously renewed with a flow-through of 50% of the total HRAP volume per day.

The same sampling strategy was carried out for ENR and SW (Fig. 1, Supplementary Table 1). Temperature was measured using a probe and pH was measured using a pH paper between 8 and 10 am every day from Monday to Friday. Every week, 500 mL water was filtered onto a GF/F filter (45 mm, Whatman, Maidstone) conserved in the dark at -20°C for Chlorophyll *a* measurement. The remaining filtrate was conserved at -20°C until nutrient analyses. To further identify *Ulva* sp.'s associated microbial diversity, samples were taken at 3 sites within each HRAP. Every week, 100 mL water was filtered onto a $0.22 \mu\text{m}$ polycarbonate filter (25 mm, Whatman, Maidstone) which was conserved at -80°C until further processing. Every two weeks, three *Ulva* thalli were randomly collected from each of the three sites. From each thallus, a surface of 22.1 cm^2 (resulting in a total surface of 44.2 cm^2 , recto and verso included) was cut, rinsed 3 times with artificial sterile sea-water (24.7 g NaCl , $6.3 \text{ g MgSO}_4\cdot 7\text{H}_2\text{O}$, $4.6 \text{ g MgCl}_2\cdot \text{H}_2\text{O}$, 0.7 g KCl) [38], and conserved at -80°C until DNA extraction of the *Ulva* biofilm.

2.2. Measurements of contextual parameters

Concentrations of nitrate, nitrite, silicate and phosphate were measured from the GF/F-filtrate following a standard automated colorimetry procedure on a continuous flow AutoAnalyser III (Seal Analytical, King's Lynn) [39,40]. The tool's detection limits were determined by measuring triplicated blanks. The detection limits were 50 nM for nitrate and silicate and 20 nM for nitrite and phosphate, calculated as the mean of the data plus three times the standard deviation (i.e., 99% confidence interval). The detection limits were well below the measurements made on the samples, which were in the μM range. Ammonium concentration was measured by fluorescence on a fluorometer TD700 (Turner Designs, San Jose) [41,42]. Chlorophyll *a* was extracted from the GF/F filters with 5 mL methanol, and measured using a Turner Design fluorometer [43].

2.3. Molecular approaches to identify the cultivated *Ulva* species and the associated bacterial diversity

To identify the cultivated *Ulva* species, DNA was extracted from grounded and lyophilized *Ulva* tissue samples taken on March 3rd, 2021 in the SW raceway. After amplification, the *rbcl* gene was identified using a Sanger sequencing approach (see Supplementary text for detailed molecular and phylogeny protocols). To survey the associated

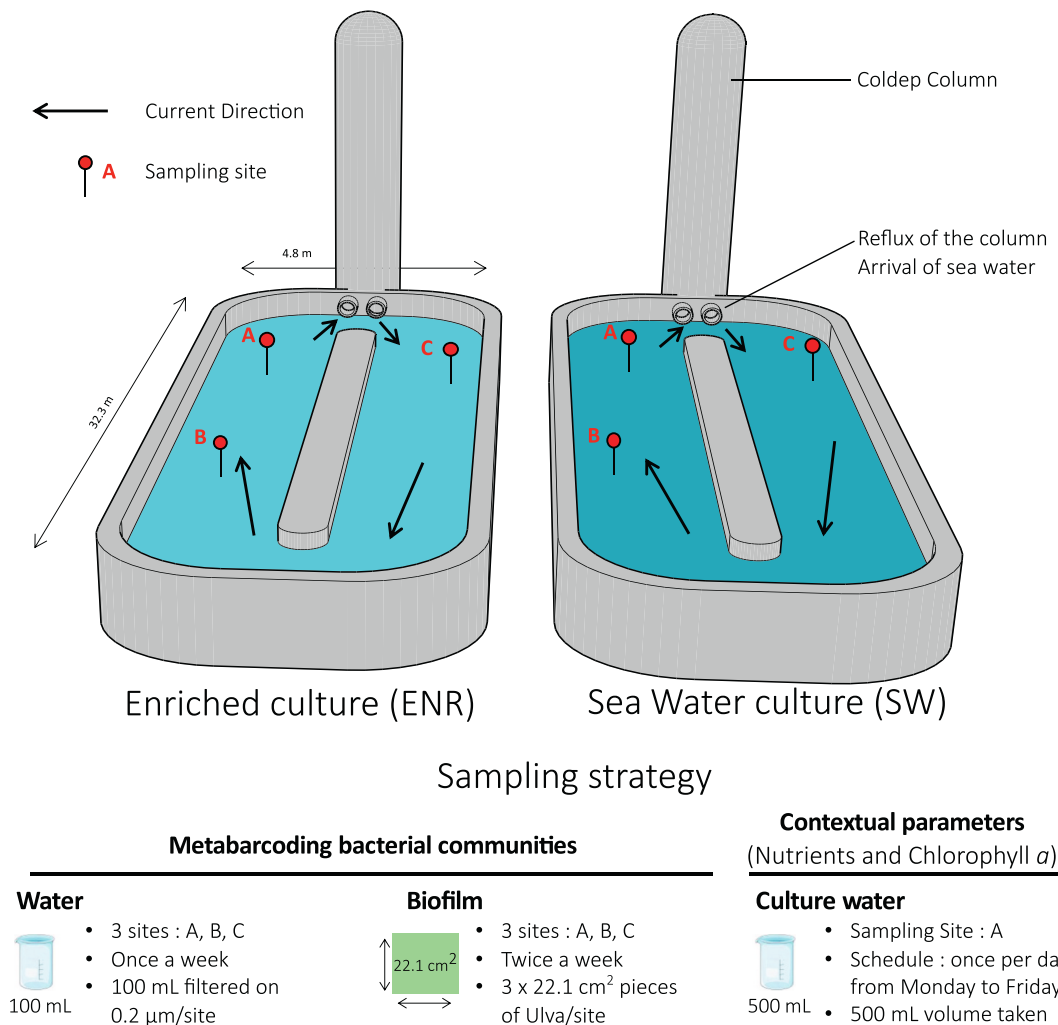


Fig. 1. Recapitulative scheme of the Coldep raceways used by ERANOVA to cultivate *Ulva* and of the sampling strategy. The two raceways were used for the enriched and seawater cultures. A brief description of the system is represented by the current direction (black arrow), the Coldep column and their backflow vents permitting water mixing, and the 3 sampling sites A, B, and C (red pointer). The sampling strategy was to sample water and *Ulva* thalli to assess the microbial diversity by metabarcoding and to measure contextual parameters (nutrients, chlorophyll *a*). Details of the sampling strategy are listed for each sampling approach.

bacterial diversity, DNA was extracted from 42 algal biofilm samples and 66 filters. Each filter was individually treated as follows: (I) cell lysis was performed by two incubation steps under vertical rotative agitation: for 45 min at 37 °C with 750 μL lysis buffer (0.75 M sucrose, 1 M Tris, 0.5 M EDTA) and 10 μL lysozyme (20 mg·mL⁻¹); and then for 1 h at 55 °C with an addition of 10 μL proteinase K (20 mg·mL⁻¹) and 50 μL SDS (20%); (II) nucleic acids were extracted by adding 1 volume of phenol-chloroform-isoamyl alcohol (PCIAA, 25:24:1) for 1 volume of lysate, and collecting the aqueous phase after 15 min of centrifugation at 4500 rpm; (III) nucleic acids were then purified using the Macherey-Nagel™ NucleoSpin™ Plant II kit by following the manufacturer's instructions from step 4 ("Adjust DNA binding conditions") to step 7 ("elute DNA") with some modifications: at step 4, where 1 volume of PC buffer was added to 1 volume of the supernatant retrieved from PCIAA purification. Step 5 was repeated until all of the mixture was bound onto the green column, and, at step 7, there was no incubation time for the second elution [1]. DNA from *Ulva* thallus pieces was extracted with the same protocol as for the filters with some modifications: (I) first, three *Ulva* thallus squares of a given sampling site altogether were immersed in 4.5 mL of cell lysis buffer and 60 μL of lysozyme; then with (II) 60 μL of proteinase K and 300 μL of SDS, and finally (III) 6 mL of PCIAA for the nucleic acids' extraction step. Also, a second extraction step was included by adding to the aqueous phase 0.3 volume of 100% ethanol,

and adding 1 volume of PCIAA before collecting the aqueous phase after 15 min of centrifugation at 4500 rpm [2]. Extracted DNA were then conserved at -20 °C until further processing. Extracted DNA were then sent to Genome Quebec (Quebec, Canada), where library preparation and 2 × 300 bp paired-end MiSeq sequencing (Illumina, San Diego, CA, USA) were carried out. For each sampling date, extracted DNA from filtered water from the 3 sites was pooled before PCR amplification whereas extracted DNA from *Ulva* thallus pieces from the 3 sites were considered individually. A metabarcoding approach targeting the V3-V4 variable region of the 16S rDNA was used to survey the bacterial communities in *Ulva* cultures. Raw sequences were deposited at the National Center for Biotechnology Information (NCBI) under the BioProject identifier PRJNA1081356. Raw 16S rDNA sequences were filtered, quality checked, curated and analyzed separately by using publicly available softwares such as cutadapt (v4.4) [44] and dada2 [45] using the R software v4.2.2 [46]. Resulting 16S rDNA amplicon sequence variants (ASV) were taxonomically annotated using Silva v138.1 [47,48]. For details, please see Supplementary text, Supplementary Table 1, and the corresponding R scripts on Github (https://github.com/Estoup/HOLOGREEN/blob/main/16S/processing_16S.R).

2.4. Multivariate and statistical analyses

Alpha-diversity indices such as the observed richness and the Shannon index were calculated from the raw sequence table (microbiome_v1.20.0 package) [49]. Alpha-diversity indices of each condition and compartment were compared with a post-hoc Dunn test (FSA_v0.9.5) [50] and *P*-values were corrected for multiple comparison with the Benjamini-Hochberg method. Before searching for beta-diversity patterns, zeros from the sequence abundance table were replaced by a Bayesian-Multiplicative replacement using the count zero multiplicative method (zCompositions_v1.4.0-1) [51], and the abundance table was then normalized using the centered log-ratio technique [52]. A distance matrix was then calculated using the Euclidean method to calculate the Aitchison distance (phyloseq_v1.42.0) [53,54]. The resulting distance matrix was then used for the three subsequent analyses: hierarchical clustering using the Ward.D method (stats_v4.2.2) [46], non-Metric MultiDimensional Scaling (nMDS), and PERmutational Multivariate ANalysis of VAriance with 1000 permutations (PERMANOVA, vegan_v2.6-4) [55]. Contextual parameters (i.e. water temperature and pH, ammonium, nitrite, nitrate, phosphate, silicate and chlorophyll *a* concentration, Supplementary Table 2) were z-score transformed (vegan_v2.6-4). On March, 30th, the chlorophyll *a* concentration in the SW water was not measured but estimated as the median value of $0.609 \mu\text{g}\cdot\text{L}^{-1}$. To identify the set of contextual parameters that best explained the variation of the bacterial community, a forward selection of the parameters was carried out on the distance matrix, based on a canonical redundancy analysis algorithm and 1000 Monte Carlo permutation tests and the Akaike Information Criterion allowed identifying the best-fitting models [56]. A redundancy analysis was then calculated from the resulting best set of contextual parameters and the distance matrix [55]. The metabolic capacities for nitrogen reduction in *Ulva* cultures were determined through metagenomic analysis using the Phylogenetic Investigation of Communities by Reconstruction of Unobserved States (PICRUST2, v2.5.2) software. ASV sequences were analyzed with this pipeline using default parameters and the Integrated Microbial Genomes (IMG) embedded database [57,58]. We used the results of Kyoto Encyclopedia of Genes and Genome (KEGG) Ortholog (KO) number assignments to investigate the nitrate reduction pathways [59–61]. Sequence processing and data analyses were done using the R software v4.2.2 [46].

3. Results

3.1. Molecular identification of the cultivated *Ulva* species

A molecular approach was used to identify the cultivated *Ulva*. Thirty-eight representative *rbcl* gene sequences of *Ulva* species from GenBank were aligned with the consensus sequence obtained from extracted DNA of the cultivated *Ulva*. A maximum likelihood tree based on 1270 positions was then constructed (Supplementary Fig. S1). The phylogeny clearly separated the sequences into four major groups, identified as I, II, III and IV, as confirmed by the bootstrap analysis (>70%). Group I was divided into three branches, including one clade (Ia) with genetically diverse taxa (sequence distances ranging from 0 to 0.25%, bootstrap values >70%), and one sequence from the species *U. clathrata* (Ib) quite divergent (0.8%) from the others within group I. Another clade was identified within group I (Ic), it included several species with highly similar *rbcl* gene sequences (sequence distances: 0–0.17%, bootstrap values <70%, Supplementary fig. S1). The *rbcl* gene sequence from the cultivated *Ulva* fell within clade Ic which also included sequences from *U. rigida*, *U. lacinulata*, *U. scandinavica* and *U. laetevirens*.

3.2. Taxonomic composition of the bacterial community

The taxonomic composition of the ASV from the algal biofilm and

water of *Ulva* cultures under SW or ENR conditions was investigated at the class level. Amongst the 31 bacterial classes identified in the entire dataset, *Gammaproteobacteria*, *Alphaproteobacteria* and *Bacteroidia* accounted for 93.8% sequences (Fig. 2, Supplementary Table 3). A distinct pattern was observed for the biofilm and the water compartments. *Gammaproteobacteria* were represented by more sequences in the biofilm (45.6% sequences) than in the water (9.7% sequences), *Alphaproteobacteria* showed similar abundances, with 31.5% and 35.4% sequences respectively, and *Bacteroidia* were less abundant in the biofilm, accounting for 14.9% sequences, compared to 52.2% in the water.

In the biofilm, the three most abundant classes were differently distributed between the two culture conditions. *Gammaproteobacteria* represented 63.5% sequences in SW and 27.8% in ENR, *Alphaproteobacteria*, 24.8% sequences in SW and 38.2% in ENR, and *Bacteroidia*, 6.1% sequences in SW and 23.7% in ENR. Differences in sequence abundance between SW and ENR were also observed at the genus level. Within *Gammaproteobacteria*, *Granulosicoccus* remained the most dominant genus in both conditions, with 42.4% of the total sequences in the biofilm in SW and 15.8% in ENR. The genus *Glaciecola* represented similar abundances in both conditions with 9.8% sequences in SW and 8.9% in ENR, and *Agaribacterium* showed higher abundances in SW with 10% sequences, compared with 0.1% in ENR. Within *Alphaproteobacteria*, the *Jannaschia* genus was dominant in the biofilm, with less sequences in SW (6.2%) than ENR (10.8%). The unassigned *Rhodobacteraceae* ASV displayed 8.6% sequences in SW and 10.5% in ENR (Fig. 2). Within *Bacteroidia*, some genera were more abundant in ENR than in SW, such as *Croceitalea* (1% sequences in SW and 8.7% in ENR), *Maribacter* (1.2% sequences in SW and 5.9% in ENR) and *Winogradskyella* (1.8% sequences in SW and 3% in ENR).

In the water, *Bacteroidia* was the predominant class in SW, representing 69.4% sequences, compared with 35% in ENR. Conversely, *Alphaproteobacteria* was more abundant in ENR (51.1% sequences) than in SW (19.7%). *Gammaproteobacteria* was represented by about 10% sequences in both conditions. Within *Bacteroidia*, *Aurantivirga* dominated SW and ENR, with 33.1% and 21.6% sequences, respectively. There were more *Polaribacter* sequences in SW (17.5%) than in ENR (5.5%). Three genera belonging to *Alphaproteobacteria*, namely, *Marivita*, *Nereida*, and *Yoonia-Loktanella*, were more abundant in ENR than in SW, with 15.7% vs. 0.8% sequences, 12.8% vs. 6.3% sequences, and 4.4% vs. 0.1% sequences, respectively. Other genera were less abundant in ENR than in SW: the NS3a marine group (0.1% sequences in ENR vs. 9.4% in SW), *Ponticoccus* (7.9% sequences vs. 0.3%), and *Polaribacter* (17.5% sequences vs. 5.5%). The bacterial diversity in *Ulva* cultures exhibited variations not only between SW and ENR but also between the biofilm and water compartments.

3.3. Temporal fluctuations of the bacterial community in the biofilm and the culture water

We investigated temporal fluctuations of the bacterial community from March 9th (D5) to May 25th (D82), in the biofilm and water in SW and ENR. The community composition and distribution were clearly different between the biofilm and the water (Fig. 2). In the biofilm, *Gammaproteobacteria* was the most abundant class in the bacterial community on D5 with an average of $86.3 \pm 8.6\%$ and $49.2 \pm 5.7\%$ sequences, in SW and ENR respectively (Fig. 3, Supplementary Table 4). *Gammaproteobacteria* decreased through the experiment, reaching about half the sequences in SW and became the least abundant class in ENR at the end of the experiment. Within this class, *Granulosicoccus* was dominating the bacterial community in SW throughout the study, and decreased from $78.1 \pm 8.4\%$ (D5) to $40.6 \pm 7.1\%$ sequences (D82). In ENR, *Granulosicoccus* was dominant from D5 to D26, with $45 \pm 6.8\%$ to $20.1 \pm 2\%$ sequences and its abundance subsequently decreased until D82. *Glaciecola* was mostly abundant from D26 to D68 in SW and ENR with about 11.5 to 9.6% and 12.4 to 6.4% sequences per date, respectively. In SW, *Agaribacterium* was mostly abundant from D5 ($4.4 \pm 3\%$

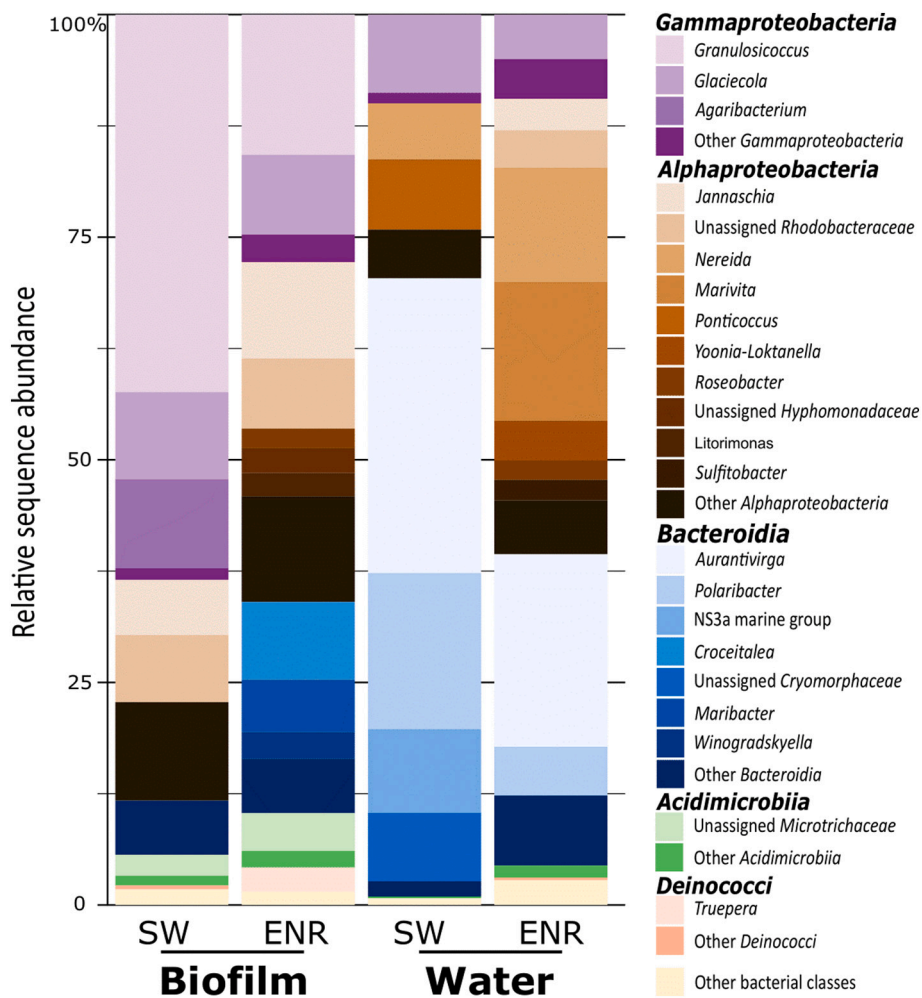


Fig. 2. Bacterial diversity at the class and genus levels in all of the *Ulva* biofilm and water samples in the two culture conditions. Relative abundance of the bacterial community at the class and the genus levels from the *Ulva* biofilm and the cultivation water in the two culture conditions for all samples combined. Genera were classified according to their class level. Genera representing less than 2% of the sequence abundance in one sample type were summed into the « Other » categories. SW, culture condition in seawater without enrichment; ENR, culture condition with a nitrate-based fertilizer enrichment; Biofilm, *Ulva* biofilm; Water, filtered cultivation water; Unassigned family name, ASV assigned only until the family taxonomic level. Others, see Supplementary Table 3 for details.

sequences) to D68 ($10.1 \pm 10.6\%$ sequences). In ENR, this genus was less abundant in the community, with about 0.3% on D5, 0.1% sequences on average throughout the experiment, and no detectable sequences on D82. In parallel, *Alphaproteobacteria* increased in sequence abundance in the two conditions through the experiment (from $6.5 \pm 3.2\%$ to $35.8 \pm 2.3\%$ sequences in SW and from $19.5 \pm 3.9\%$ to $51.4 \pm 3.5\%$ sequences in ENR). In SW, the *Jannaschia* genus was mostly abundant from D41 ($14.3 \pm 6.2\%$) to D82 ($7.6 \pm 0.5\%$). In ENR, *Jannaschia* was most abundant earlier in the experiment, from D26 with $7.9 \pm 2.4\%$ to D68 with $26.5 \pm 4.4\%$ sequences. While not present in SW or in very low abundance, *Litorimonas* and *Roseobacter* were abundant genera in ENR with about 2.5% sequences on average throughout the experiment. Throughout the experiment, *Bacteroidia* was less abundant in SW ($6.1 \pm 1.8\%$ sequences on average) compared to ENR ($23.7 \pm 2.5\%$ sequences on average). The *Croceitalea* genus was not abundant in SW, with about 1% sequences on average compared to ENR with abundances of $21 \pm 3.6\%$ sequences on D26 to $6.2 \pm 4.5\%$ sequences on D82. *Maribacter* was not abundant in SW ($1.2 \pm 0.6\%$ sequences on average) but it was more abundant in ENR, with fluctuations ranging from $4 \pm 1.2\%$ to $8.4 \pm 1.7\%$ per sampling date. *Winogradskyella* was notably abundant in SW at D54 and D68 with about 4% sequences, and was also observed in ENR at the same dates with $6.9 \pm 2\%$ and $5.5 \pm 2.1\%$ sequences. To evaluate the ASV fluctuations through the

experiment, the mean of the standard deviations (SD) of the sequence abundances of each ASV from the biofilm was calculated within a culture condition. The obtained value was significantly higher in ENR (total ASV SD mean of 5.8×10^{-2}) than in SW (total ASV SD mean of 4.2×10^{-2} for SW, Post-hoc Dunn test, $P = 7.7 \times 10^{-6}$), suggesting larger ASV fluctuations in ENR than in SW. In both conditions, the bacterial community composition and genus equitability in the biofilm were varying through time and were clearly affected in ENR five days after the first addition of nitrate-based fertilizer to the *Ulva* culture. Fertilizer addition along with water renewal led to a stable bacterial composition from D26-D41, the most abundant genera distributed more equitably at D54, and the bacterial community mostly composed of less abundant genera at D82.

In the water, *Bacteroidia* dominated the community in all SW samples, with 47% to 80.4% sequences throughout the experiment (Fig. 4, Supplementary Table 5). *Bacteroidia* was less abundant in ENR, with fluctuations from 26.1% to 70% sequences. Within *Bacteroidia*, *Aurantivirga* increased from 2.2% sequences on D5 to 51.5% on D68 in SW while its sequence abundance in ENR fluctuated throughout the experiment from 2.4 to 45.4% sequences. The genus *Polaribacter* fluctuated from 4.5 to 50.4% sequences in SW and from 2.9 to 18.4% in ENR. NS3a marine group's abundance decreased in SW from 30.1% sequences on D5 to 0.5% on D82 and was present in ENR in very low sequence

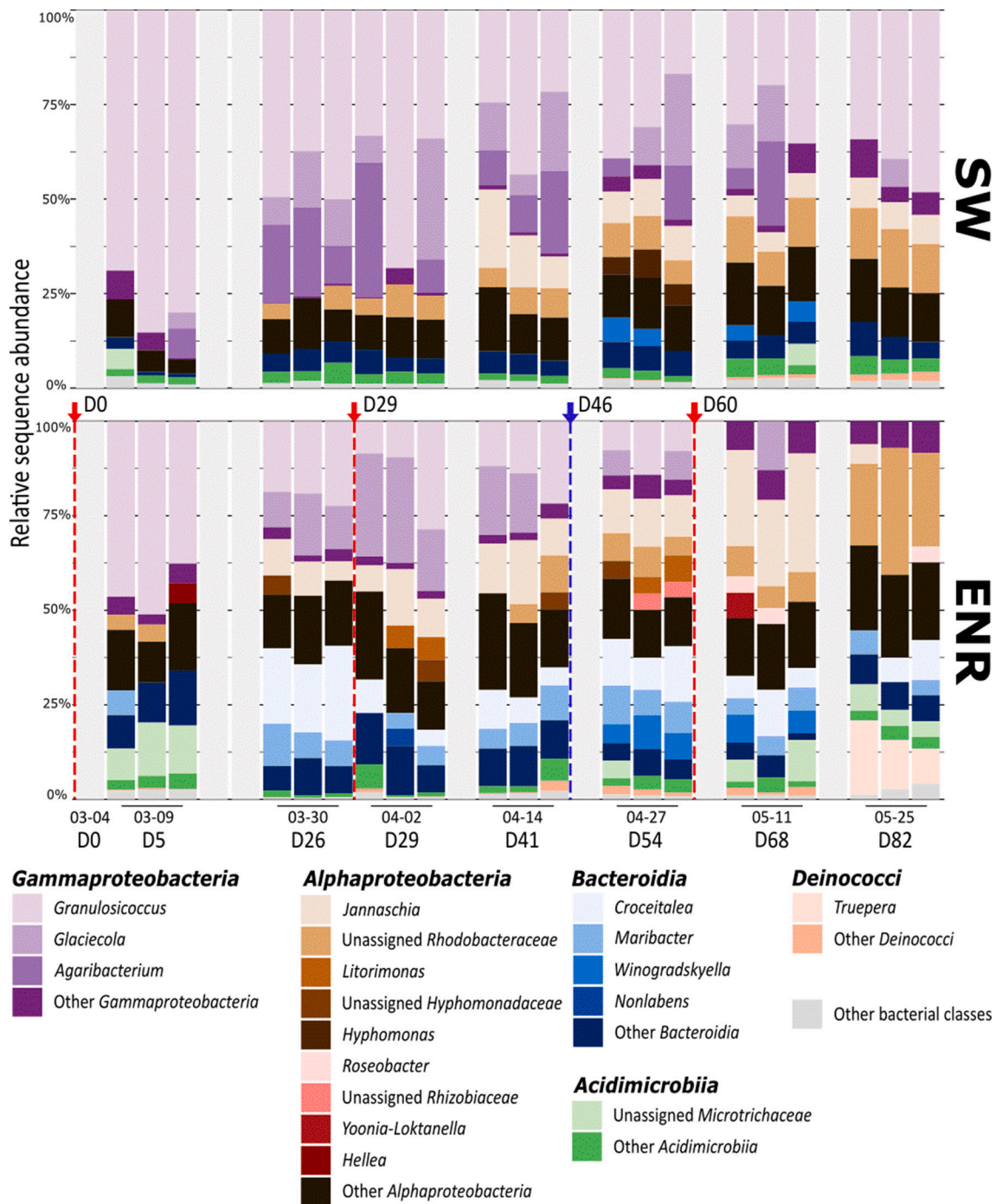


Fig. 3. Temporal fluctuations of the bacterial community in the *Ulva* biofilm. Relative abundance of the bacterial community was investigated at the class and genus levels within the *Ulva* biofilm over 12 weeks (from March, 3rd to May, 25th 2021) under two culture conditions (SW and ENR). Genera were classified according to their class level. Genera representing less than 4% of the sequence abundance in each sample were grouped into “Other” (see Supplementary table 4 for details). Unassigned genera were assigned to the lowest identified taxonomic level. For each date (numbered from day 0, D0, to day 82, D82), sampling was performed in triplicate. Grey bars indicate weeks without sampling. The red dashed line in the ENR section indicates water culture renewal and a subsequent fertilization event between two sampling dates. The blue dashed line in the ENR section indicates a water culture renewal between two sampling dates without addition of fertilizer.

abundance at few sampling dates. *Alphaproteobacteria* were less abundant in SW than in ENR, ranging from 22.1% to 17.3% sequences and from 54.7% to 21.2% sequences between D5 and D82, and were different in genus composition. *Nereida* remained present in SW with 14.1% sequences on D5 and 4.3% on D82 while it fluctuated in ENR with highest abundances from D41 to D54. *Marivita* was low abundant in SW with a peak at 5.9% sequences on D47 and fluctuated in ENR with highest abundances from D26-D34 (42.9–67.2% sequences). In SW,

Ponticoccus was mostly abundant from D41-D82 with 5.5–18.1% sequences but it was only detectable in ENR in the final two weeks, with 0.02–3.1% sequences. *Gammaproteobacteria* showed distinct fluctuations between the two conditions. *Glaciecola* was most abundant in SW at the beginning of the experiment D5-D29 (11.9–27.5% sequences), and was fluctuating in ENR, from 1.7 to 12.3% throughout the experiment. In the water, there were significantly higher ASV fluctuations in ENR compared to SW (Post-hoc Dunn test, $P = 2.6 \times 10^{-26}$, total ASV SD

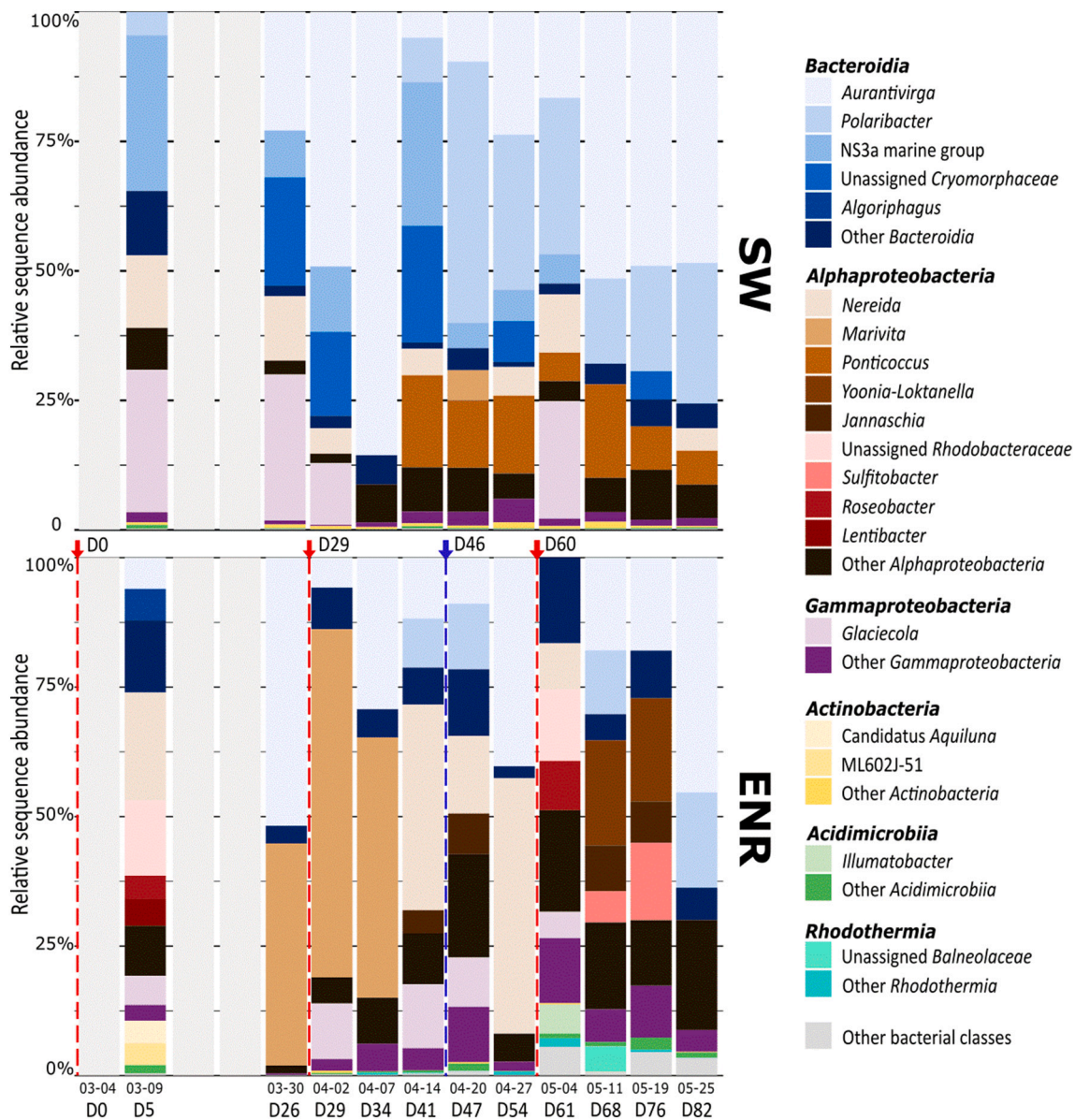


Fig. 4. Temporal fluctuations of the bacterial community in the cultivation water. Relative abundance of the bacterial community was investigated at the class and genus levels in the *Ulva* biofilm over 12 weeks (from March, 3rd to May, 25th 2021) under two culture conditions (SW and ENR). Genera were classified according to their class level. Genera representing less than 4% of the sequence abundance in each sample were grouped into “Other” (see Supplementary table 5 for details). Unassigned genera were assigned to the lowest identified taxonomic level. Each date was numbered from day 0, D0, to day 82, D82. Grey bars indicate weeks without sampling. The red dashed line in the ENR section indicates water renewal and a subsequent fertilization between two sampling dates. The blue dashed line in the ENR section indicates water culture renewal between two sampling dates without addition of fertilizer.

mean of 5.6×10^{-2} for SW vs. 8.0×10^{-2} for ENR). The bacterial community composition and equitability in ENR differed from SW after five days. The addition of a nitrate-based fertilizer coupled with water renewal in the raceway at D28 and D60 seemed to impact the bacterial community composition.

3.4. Diversity patterns of the bacterial community

Alpha-diversity was surveyed for all samples by calculating the observed richness and the Shannon index (Fig. 5A, Supplementary Table 6). No significant difference was observed between the mean of the observed richness of the two culture conditions for the two compartments (SW biofilm vs. ENR biofilm and SW water vs. ENR water, $P = 0.365$, $P = 0.079$, respectively; Supplementary Table 7). The mean of the Shannon index in the ENR biofilm was significantly higher than in the

SW biofilm and this trend was also observed in the water compartment ($P = 3.6 \times 10^{-2}$, $P = 2.8 \times 10^{-2}$, respectively). There was a significant mean difference between the Shannon index of the SW biofilm and the SW water but no significant difference between the ENR biofilm and the ENR water ($P = 4.6 \times 10^{-2}$, $P = 0.1$, respectively).

Pairwise comparisons of the bacterial community in biofilm or water samples for the two conditions were calculated with Aitchison distances and using clustering and ordination to identify potential discontinuous and continuous patterns (Fig. 5B, Supplementary Fig. S2). Hierarchical clustering allowed distinguishing five clusters representing samples from the SW biofilm and ENR biofilm at the beginning of the experiment (March, 9th, 30th and April, 2nd, corresponding to D5, D26 and D29, cluster 5), SW biofilm samples (cluster 4), ENR biofilm samples (cluster 3), SW water samples (cluster 1) and ENR water samples (cluster 2). Compartment type and culture condition had a strong impact on the

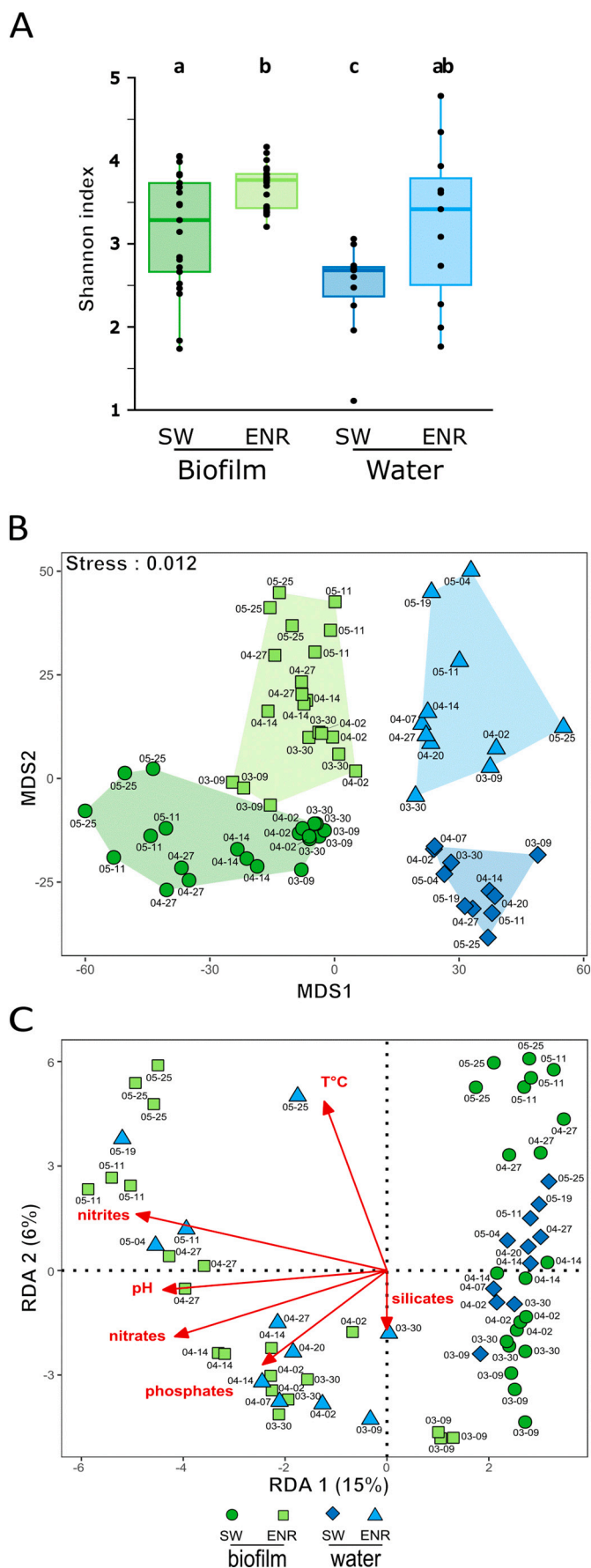


Fig. 5. Diversity of the bacterial community of the *Ulva* biofilm and cultivation water in the two culture conditions from March, 9th to May, 25th 2021. Shannon index of all the samples in the two compartments for the two conditions (A). A letter above a boxplot indicates a significantly different mean (Post Hoc Dunn test: Adj. p -value < 0.05) between compartments and conditions. Non-Metric Multidimensional Scaling (nMDS) was conducted based on Aitchison distances between samples at the ASV level (B). Colored shapes represent each compartment within each condition. Redundancy analysis (RDA) of the bacterial community based on the calculation of Aitchison distances between samples at the ASV level and constrained by six contextual parameters (C). SW, culture condition in seawater without enrichment; ENR, culture condition with a nitrate-based fertilizer enrichment; biofilm, *Ulva* biofilm; and water, filtered cultivation water; T°C, water temperature; pH, water pH; nitrite, nitrite concentration in the water; nitrate, nitrate concentration in the water; phosphate, phosphate concentration in the water; silicates, silicates concentration in the water. MM-DD, sampling dates indicated by following this notation: month-day.

structuring of the bacterial community (permutational analysis of variance, PERMANOVA, $F_{3,60} = 12.6$, $P < 0.001$, Fig. 5B), as significant differences were observed from pairwise comparisons of biofilm and water samples for SW and ENR (PERMANOVA, ENR biofilm vs. SW biofilm, $F_{1,40} = 12.2$, $P < 0.001$; ENR biofilm vs. ENR water, $F_{1,30} = 7.5$, $P < 0.001$; ENR water vs. SW water, $F_{1,20} = 7.4$, $P < 0.001$; Supplementary Table 8). For each compartment within each condition, closer dates tended to cluster together by hierarchical clustering and a temporal gradient could be observed on the nMDS with samples being further from each other as they were taken later on (Fig. 5B). The hierarchical clustering of biofilm triplicates underlined not only the reproducibility of our sampling approach, but also the relative homogeneity of the microbiota at the surface of distinct *Ulva* individuals. Overall, the bacterial community structure was specific to each compartment and culture condition and bacterial diversity was also structured according to time.

A forward selection analysis allowed identifying nitrite, nitrate, phosphate, silicate, pH and water temperature as significant explanatory contextual parameters ($P < 0.05$) influencing bacterial community structure. A subsequent redundancy analysis (RDA) revealed that these parameters accounted for 29.3% of the total variance observed in the community structure, with 15.1% and 6.2% of the variance explained by the two first RDA axes (Fig. 5C, Supplementary Table 9). SW samples were associated with lower concentrations of nitrites, nitrates, phosphates, and lower pH, while ENR samples were associated with higher concentrations of these nutrients and of the pH. As the experiment proceeded, ENR and SW samples were associated with higher temperatures. Each of the two compartments was similarly impacted by contextual parameters and the temporality of samples from both conditions was clearly related to temperature.

3.5. Shared, unique ASV and the core microbiota in *Ulva* cultures

We searched for the common ASV to the two culture conditions that were present in at least one sample in the biofilm and in the water and for unique ASV to each compartment. In the biofilm, while 46% ASV (corresponding to 583 ASV and representing 97.3% sequences) were shared between SW and ENR, 36% ASV (1.6% sequences) were unique to SW and 18% ASV (1.1% sequences) to ENR (Fig. 6). In the water, 46% ASV (208 ASV, 93.5% sequences) were shared between SW and ENR, 18% ASV (17.5% sequences) were unique to SW and 36% (36.1% sequences) to ENR. The core microbiota for each compartment was determined by identifying the ASV present in every sample, regardless of the culture condition or the date of sampling (Fig. 7, Supplementary table 10). The core microbiota of the biofilm was represented by 17 ASV, which accounted for 51.2% of all the sequences in this compartment. Within this core, the *Gammaproteobacteria* genus *Granulosicoccus* accounted for 49% sequences. In *Bacteroidia*, *Croceitalea* and *Maribacter*

(caption on next column)

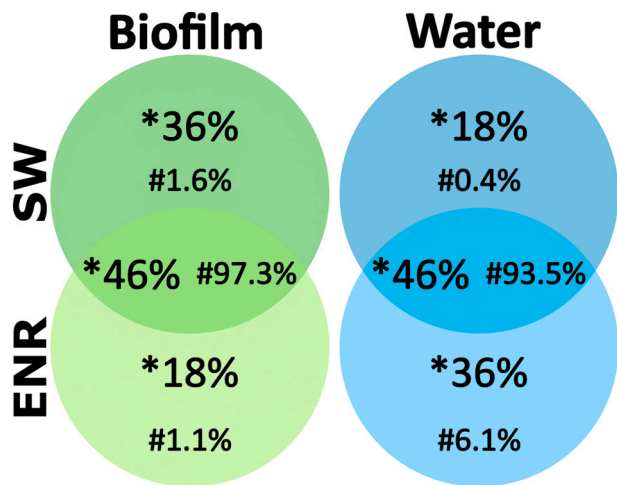


Fig. 6. Number of shared and unique ASV between all samples from the biofilm and the water in SW and ENR. *, relative ASV abundance; #, relative sequence abundance.

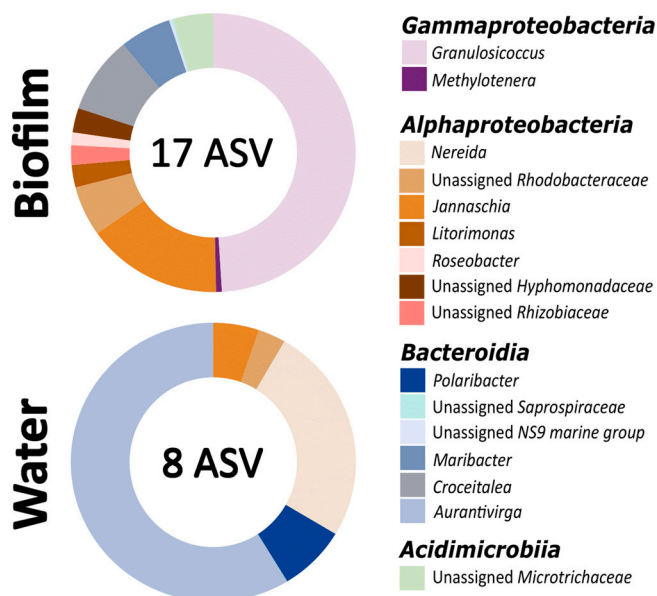


Fig. 7. Taxonomic composition of the core microbiome shared between all SW and ENR samples in the biofilm and in the water. The relative sequence abundance of the 17 core ASV from the biofilm accounted for 51.2% of the total sequence abundance in the biofilm samples. The relative sequence abundance of the 8 core ASV from the water accounted for 39.8% of the total sequence abundance in the water samples. Genera were classified according to their respective class levels (see Supplementary table 10 for more details). Unassigned genera were assigned to the lowest identified taxonomic level.

represented 8.9% and 5.9% core sequences, respectively. In *Alphaproteobacteria*, the *Jannaschia* genus represented 15.5% core sequences and the unassigned *Rhodobacteraceae* ASV, 5.8% sequences. In the water, the core microbiota was represented by 8 ASV, corresponding to 39.8% water sequences. These 8 ASV were classified as *Bacteroidia*, with *Aurantivirga* dominating the core microbiota with 58.7% core sequences, followed by *Polaribacter* with 7.7% sequences. In *Alphaproteobacteria*, *Nereida* represented 25.3% core sequences.

3.6. Nitrogen metabolic capacity of microbial communities with and without fertilization

The effect of nitrate-based fertilizer addition to *Ulva* cultures on the potential metabolism of the bacterial community was assessed in the biofilm and in the water. ASV assigned to taxa encoding enzymes involved in three core nitrate reduction pathways (Supplementary fig. S3) were identified using PICRUSt2 [57]. For each metabolic step, sequence abundances for every ASV associated with the relevant enzymes were summed per sample to calculate the sample's reaction relative abundance (SRRRA). The differences in SRRRA values between ENR and SW were then calculated for each sampling date, with the biofilm and water treated separately, to measure the prevalence bias of the metabolic reaction in SW or ENR (Fig. 8, Supplementary Table 11). We called the result of this difference the prevalence bias index $PBI = SRRRA_{ENR} - SRRRA_{SW}$.

The dissimilatory reduction of nitrate to ammonium (DNRA) and the denitrification pathways begin with nitrate reduction to nitrite by nitrate reductases (*narGHI*, *napAB*, Supplementary Fig. S3). Amplicon sequence variants assigned to taxa encoding nitrate reductases were more abundant in the SW biofilm than in the ENR biofilm almost throughout the experiment. This was shown by negative PBI values for all dates but D82, for which the difference in sequence abundance was slightly higher (by 0.6 points) in ENR (Fig. 8A). The DNRA pathway follows by nitrite reduction to ammonium by nitrite reductases (*nirBD* or *nrFAH*). The PBI distribution for these enzymes was characterized by a range of both negative and positive values indicating that SW and ENR contained similar sequence abundances of taxa encoding this metabolic step in the biofilm. The denitrification pathway converts nitrite to dinitrogen in 3 successive steps using nitrite reductases (*nirK* and *nirS*; nitrite→nitric oxide), nitric oxide reductase (*norBC*; nitric oxide→nitrous oxide) and nitrous oxide reductase (*nosZ*; nitrous oxide→dinitrogen). These three reactions contained only positive PBI values in the biofilm as taxa capable of supporting the denitrification pathway were globally more abundant in ENR than in SW. The most substantial difference concerned the nitrous oxide to dinitrogen step, with an average increase in sequence abundance of 17.8 points in ENR. On average, taxa encoding *nosZ* represented 22.2% and 4.5% sequences in ENR and SW, respectively. In contrast, preliminary steps of the denitrification pathway encoded 2.4%, 5.3%, and 3.4% sequences in ENR and 11%, 1.7%, and 1.2% sequences in SW for the nitrate to nitrite, nitrite to nitric oxide, and nitric oxide to nitrous oxide steps, respectively. Finally, the assimilatory nitrate reduction to ammonium (ANRA) pathway comprises two metabolic steps carried out by assimilatory nitrate reductases (*narB*, *NR*, *nasAB*; nitrate→nitrite) and assimilatory nitrite reductases (*nit-6*, *nirA*, *nasBDE*; nitrite→ammonium). The assimilatory nitrate reductase step showed a distribution of negative and positive PBI values, arguing against a systematic overabundance of taxa responsible for this metabolic step in the biofilm in SW or ENR (Fig. 8A). The nitrite reductase step, however, was characterized by a distribution of exclusively positive, albeit low, PBI values in ENR (average PBI = 0.4 points). The low values were mainly explained by the low sequence abundance of the corresponding taxa (i.e., about 0.5% and 0.1% sequences on average for ENR and SW, respectively), rather than by a slight imbalance in sequence abundances between ENR and SW (Supplementary Table 11). Fertilization may thus be associated with a small but still measurable increase in sequence abundance of bacteria encoding assimilatory nitrite reductases in the biofilm.

The same approach was used to investigate the effect of fertilization on the functioning of the bacterial community in the water (Fig. 8B). For all 7 enzymatic reactions involved in the three nitrate reduction pathways, the associated distributions mainly featured positive PBI values, indicating that fertilization tended to induce a generalized sequence overabundance of taxa metabolizing nitrate and its downstream reduced derivatives. In the water, taxa capable of reducing nitrate to nitrite via the DNRA or denitrification pathways were more prevalent in ENR,

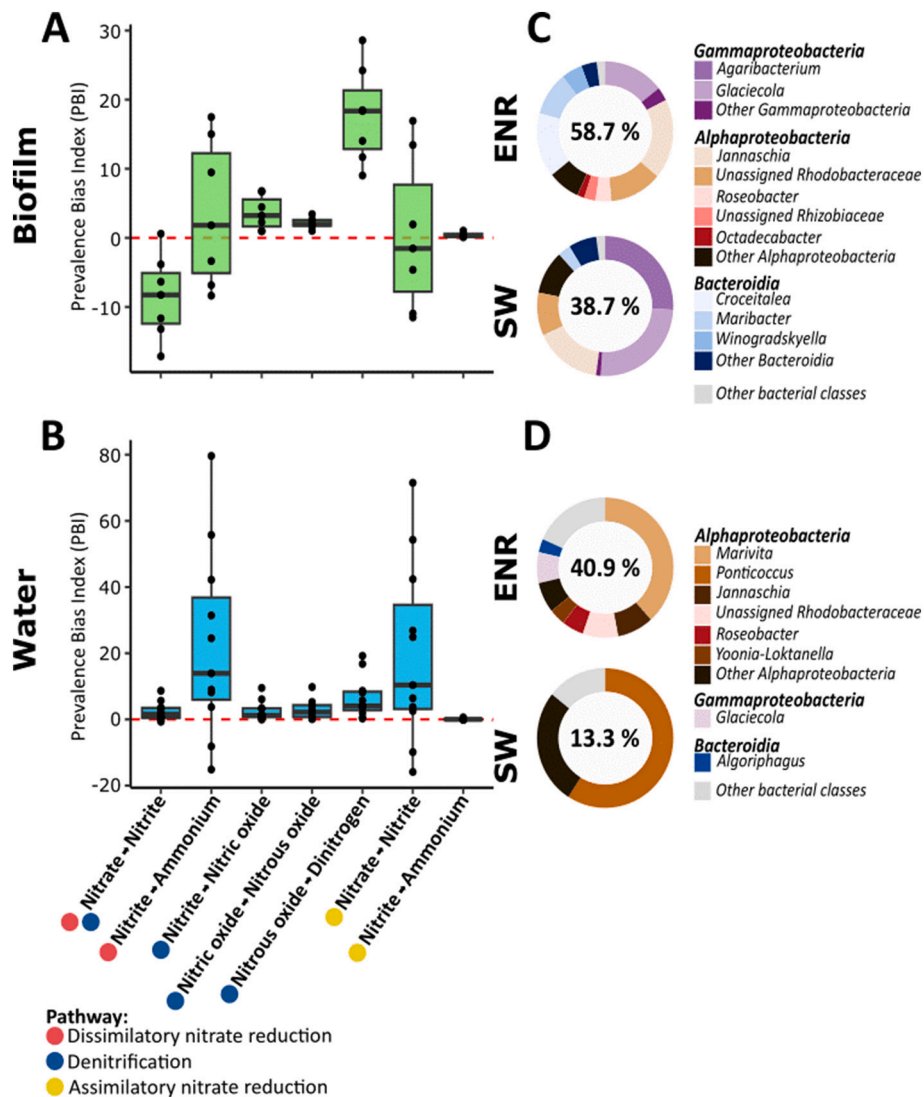


Fig. 8. Sequence abundance difference and taxonomic assignment of bacterial ASV assigned to taxa encoding nitrate reduction enzymatic reactions. The prevalence bias index (PBI) for 7 metabolic steps involved in three nitrate reduction pathways was calculated for each sampling date (black dots) in the biofilm (A) and in the water (B). For the biofilm, the mean abundance of each ASV from sample triplicates was calculated for each date before calculating differences in sequence abundance between SW and ENR. A positive value in a given reaction and compartment signifies higher sequence abundance in ENR compared to SW, whereas a negative value indicates a lower abundance in ENR. The nitrate reduction pathways are as described in the Kyoto Encyclopedia of Genes and Genomes (KEGG): dissimilatory nitrate reductase (red circles), denitrification (blue circles) and assimilatory nitrate reductase (yellow circles, Supplementary fig. S3). Taxonomic assignment and relative sequence abundance of ASV associated with nitrate reduction pathways (any of the 7 reaction steps) in the biofilm (C) and in the water (D) of the two conditions. Genera representing less than 1% of the sequence abundance in each sample were grouped into “Other” (see Supplementary table 12 for details). Unassigned genera were assigned to the lowest identified taxonomic level. SW, culture condition in seawater without enrichment; ENR, culture condition with a nitrate-based fertilizer enrichment; biofilm, *Ulva* biofilm; and water, filtered cultivation water.

whereas the biofilm compartment showed a reversed trend with an increase in sequence abundance in SW. Furthermore, the sequence abundance increase of taxa coding for the dissimilatory reduction of nitrite to ammonium was more marked in the water than in the biofilm (average PBI = 22.3% and 3.6% sequences, respectively, Supplementary Table 11). However, the reduction of nitrous oxide to dinitrogen was less abundant in the water than in the biofilm (average PBI = 6.6% and 17.8% sequences, respectively).

The taxonomic composition of the ASV associated with nitrate reduction pathways in the biofilm and water was investigated in the two conditions (Fig. 8C–D, Supplementary Table 12). In the biofilm, there were higher sequence abundances in ENR (58.7% of all sequences in ENR biofilm) than in SW (38.7% sequences) but a similar genus diversity (108 and 111 genera, respectively, Fig. 8C). Within *Gammaproteobacteria*, *Agaribacterium* and *Glaciecola* were the predominant genera in SW,

accounting for about 25–26% sequences of the ASV associated with nitrate reduction pathways. In ENR, *Glaciecola* was the most dominant *Gammaproteobacteria* genus with 14.4% sequences. Within *Alphaproteobacteria*, the most abundant genera were *Jannaschia*, with 16% sequences in SW and 18.5% in ENR, and the “unassigned *Rhodobacteraceae*” ASV, with 9.9% sequences in SW and 12.5% in ENR. The most abundant *Bacteroidia* in ENR, *Croceitalea* and *Maribacter*, accounted for 14.9% and 10.1% sequences, respectively. In the water, ASV involved in nitrate metabolism represented more sequences and more genera in ENR (40.9% sequences and 189 genera) than in SW (13.3% sequences and 165 genera, Fig. 8D). Within *Alphaproteobacteria*, the most abundant genus was *Ponticoccus* in SW with 59.1% sequences and *Marivita* in ENR with 38.3% sequences. In ENR, *Glaciecola* accounted for 7.1% sequences and the *Bacteroidia* *Algoriphagus* for 3.1% sequences. These two taxa were low abundant or absent in SW.

4. Discussion

Previous studies have primarily investigated the bacterial microbiota of *Ulva*'s biofilm in natural habitats [62–64]. Studies on microbial dynamics in *Ulva* cultures showed the influence of aquaculture practices on microbial community structure [31,35,65]. However, to our knowledge, the specific effect of nitrate-based fertilizer addition in *Ulva* cultures over time remains underexplored. Here, we compared bacterial community diversity and succession in *Ulva* cultivation with (ENR) and without (SW) fertilization over twelve weeks, by identifying its potential impact on the bacterial community functioning.

4.1. Phylogenetic position of the cultivated *Ulva* within the genus

As the visual identification of *Ulva* was not possible due to the morphological plasticity of this algal genus [66,67], we used a phylogenetic approach based on the chloroplastic *rbcl* gene to identify the species (Supplementary fig. S1). The *rbcl* gene sequence from the cultivated *Ulva* belonged to the same clade Ic and was highly similar to those from *U. rigida*, *U. lacunculata*, *U. scandinavica* and *U. laetevirens*. Previous studies investigating *Ulva* diversity based on genes such as *rbcl*, *tufA* or ITS could not obtain sequences divergent enough to distinguish *U. rigida* from *U. laetevirens* [68,69]. The species *U. laetevirens* Areschoug 1854 was thus proposed to be considered a synonym of *U. rigida* C. Agardh 1823 [69]. In the same study, *rbcl* gene-based phylogeny also led to highly similar sequences from *U. lacunculata* and *U. rigida*. In the clade Ic, there was also a *rbcl* sequence identified as *U. scandinavica* which can be considered as a synonym of *U. lacunculata* [70,71]. An additional study analyzing the plastid genome, *rbcl* and *tufA* genes and ITS sequences of *U. rigida* and *U. lacunculata* allowed highlighting the misapplication of some names attributed to *Ulva* sequences in GenBank [70]. From these analyses, they concluded that *rbcl* gene sequences identified as *U. rigida*, *U. lacunculata*, *U. scandinavica* and *U. laetevirens* clustering together, similarly as in our study, were all belonging to the species *U. lacunculata*. This suggests that the cultivated *Ulva* in our study likely belongs to the species *U. lacunculata*.

4.2. Effect of fertilizer addition on the bacterial diversity and succession patterns in *Ulva lacunculata* cultures

Despite coming from the same *Ulva* inoculum, the bacterial community associated with *Ulva*'s cultures showed a different community structure between the two culture conditions, and this was observed for both the biofilm and water compartment. These patterns were explained by temperature and pH fluctuations and the nutrient content as described by nitrites, nitrates and phosphates concentrations (Fig. 5) and suggest an adapted bacterial community to specific environmental conditions.

Over the twelve weeks, bacterial classes from the biofilm of *Ulva* cultures in SW were in majority *Gammaproteobacteria* and *Alphaproteobacteria*, phyla commonly found associated with macroalgae, regardless of the algal type (i.e. brown, red, green algae) [16,72]. More specifically, these bacterial classes were seen in the *Ulva* microbiota from the coast of several part of the world such as Australia, the Netherlands, and Columbia and at different seasons [62,63,73]. Amongst the most abundant genera of the biofilm, we found *Granulosicoccus*, *Glaciecola*, some *Rhodobacteraceae* such as *Jannaschia* and an unassigned ASV, as commonly reported in bacterial communities associated with other Ulvophyceae genera such as *U. australis*, *U. lacunculata*, *U. lactuca*, *U. linza*, or *Blidingia* from the environment [63,64,73,74]. The bacterial community fluctuated between March and May, starting with a community mainly composed of *Granulosicoccus* and low abundant genera (i.e. represented by less than 4% sequences per sample) belonging to *Alphaproteobacteria* and *Acidimicrobiia*. Throughout the experiment, other genera became represented by higher sequence abundances, including *Jannaschia* and an unassigned *Rhodobacteraceae* ASV, and an

increase in low abundant genera belonging to the five most abundant classes was observed, making the community more diverse. This was also observed at the ASV level, where there was a gain in ASV number and a higher Shannon index between the beginning and the end of the experiment.

Throughout the experiment in the ENR biofilm, the bacterial community composition and distribution were different from that from SW. This was observed at the class level, where the dominant groups were not only *Gammaproteobacteria* and *Alphaproteobacteria* but also *Bacteroidia*, as observed in IMTA systems with cultivated *U. fasciata* and *U. rigida* fertilized by fish effluents [35,65]. These classes were mostly composed of the same genera as observed in SW but also *Croceitalea*, *Maribacter*, *Winogradskyella*, and *Truepera*. In IMTA conditions, *Glaciecola*, *Granulosicoccus*, and unclassified *Rhodobacteraceae*, representing about 57% sequences altogether, were also amongst the most abundant genera associated with *U. rigida*'s biofilm [65], while the biofilm of *U. fasciata* in similar conditions was dominated by not only *Granulosicoccus* but also *Blastopirellula*, *Erythrobacter* and *Truepera*, representing about 42% of the community [35]. *Ulva* culture conditions of these two IMTA studies and our experiment presented some differences in bacterial composition which may be due to the *Ulva* species cultivated, its physiology, as well as the culture conditions, as for instance, nitrate concentration in the tanks were very different: 5 mg·L⁻¹, less than 0.9 mg·L⁻¹ and 2–192 mg·L⁻¹ in the studies from Ghaderiardakani et al. [31], Nguyen et al. [35], and our study, respectively. Additionally, we used a batch distribution of an artificial fertilizer, while the two IMTA studies used continuously distributed fish effluents, also inherently richer in organic complexity.

After 5 days of the first nitrate-based fertilization (Nitrates = 170 mg·L⁻¹), the bacterial community composition and distribution in the ENR biofilm was already different to that from SW. At the genus level at D5, *Granulosicoccus* represented less than half of the bacterial community which was also composed of some unassigned *Rhodobacteraceae* and *Microtrichaceae* ASV and low abundant *Gammaproteobacteria*, *Alphaproteobacteria*, *Bacteroidia* and *Acidimicrobiia* genera. Over the twelve weeks, dominating genera were highly fluctuating in ENR in parallel to nitrates concentrations, with at D26 (Nitrates = 35 mg·L⁻¹), *Granulosicoccus*, *Glaciecola*, *Jannaschia*, *Croceitalea*, and *Maribacter*, dominating the community, at D54 with nutrients being more diluted (Nitrates = 2 mg·L⁻¹), an increasing abundance of *Litorimonas* and *Winogradskyella*, and at D82 after the last fertilization (Nitrates = 68 mg·L⁻¹), some unassigned *Rhodobacteraceae* and *Microtrichaceae* ASV, *Croceitalea*, *Maribacter*, *Truepera*, and mostly less abundant genera (representing about 42% sequences). Such rapid fluctuations in genus composition and sequence abundance in the ENR biofilm were also observed at the ASV level. There was an increasing diversity towards the end of the experiment as described by the Shannon index and by the increasing overall standard deviation of ASV. Compared to SW, the ASV richness and overall standard deviation were higher in ENR and the bacterial community at the genus level fluctuated more, which was likely a result of the fertilization in a batch setting. This rapid succession of bacteria in ENR suggests rapid and high fluctuations of the environmental conditions of the ecological niches at the surface of *Ulva*, as observed for the green algae *Caulerpa* [75,76]. In the IMTA study from Nguyen et al. [35], the bacterial community was much more stable with time, suggesting a clear impact of the batch distribution of the fertilizer on the bacterial community compared to a continuous distribution of fish effluents. In our batch setting, the physiology of the *Ulva* holobiont was likely impacted [76], and probably adapted to these specific environmental conditions by selecting beneficial bacteria in its biofilm, as suggested by the “microbial gardening” concept [22,23].

In the wild, it has been established that bacterial communities differ between algal biofilms and the surrounding seawater, as seen with various molecular tools (e.g. denaturing gradient gel electrophoresis, clone libraries, long-reads nanopore sequencing) [62,73,77]. This was also confirmed in our culture conditions as the bacterial community

composition in the water was clearly different from the biofilm. Also, in the coastal ocean, larger concentrations of nutrients in the water have been shown to influence the bacterial community composition [78,79]. Here, the impact of fertilization on the bacterial community was observed starting at the class level, with the SW water mainly composed of *Bacteroidia* (about 69% in total), *Alphaproteobacteria* (20%), *Gammaproteobacteria* (10%), and the ENR water, mainly composed of *Alphaproteobacteria* (about 51%), *Bacteroidia* (35%), and *Gammaproteobacteria* (9.5%). Over the twelve weeks, the bacterial community in SW was mainly composed of the same genera fluctuating through the experiment, with, for instance, *Aurantivirga*, *Polaribacter*, NS3a marine group, unassigned *Cryomorphaceae* ASV, *Ponticoccus*, and *Glaciecola*. Higher fluctuations were observed in ENR, where less genera dominated the community (e.g. *Aurantivirga*, *Polaribacter*, Other *Bacteroidia*, *Nereida*, *Marivita*). There was a clear impact of fertilization from D5 on, with a very different community from SW with the dominating genera being replaced by other dominating genera at D26, D41, D61, D68, D82. These shifts in bacterial community composition were not happening at the same time as the ones from the ENR biofilm, as there were rather more drastic and more frequent. Moreover, compared to SW, the bacterial community in the ENR water was reactive to fertilization despite the batch approach.

4.3. Exploring the persistence and the functioning of the bacterial microbiota in the *Ulva* holobiont

Persistent bacteria associated with an algal host in different environmental conditions likely play a major role in the host fitness and resilience and may be defined as a core microbiota [80]. In the case of the green algae *Caulerpa*, 325 Operational Taxonomic Units (OTU) were shared between *C. cylindracea* and *C. prolifera*, including their 3 morphological niches [75]. The epiphytic microbiota from *Ulva lactuca* collected at the Colombian coast in three successive years shared 5638 OTU [63]. Here, in the biofilm, there were 583 ASV, representing 97% sequences, shared between the SW and ENR conditions, all samples pooled together (Fig. 6). Different threshold may be chosen to define core microbiota such as the presence of some ASV or genes associated with all hosts within an ecosystem [81]. Here, we defined the core microbiota as the 17 ASV found in all biofilm samples, both conditions included, representing 51% sequences (Fig. 7). The corresponding identified genera included *Granulosicoccus*, also found in the core microbiota of *Ulva fenestrata* [64], to degrade algal polysaccharides and to produce and provide vitamin B12 to the algal host [82]. We also identified *Jannaschia*, also found in the core microbiota of six *Ulvo*-phyceae species collected from the Baltic to the North Sea [64]. *Maribacter* and *Roseobacter*, part of the microbiota, are known to produce factors (AGMPFs) inducing morphogenesis of *Ulva* and to be enriched in fertilized aquaculture water [28,29,31,83], as observed in the current study. *Roseobacter* is also known to excrete antifouling compounds at the surface of *U. australis* [84]. In the water, there were 208 ASV (93.5% sequences) shared between the two conditions, while 8 ASV (40% sequences) represented the core microbiota of the cultivation water. This core microbiota contained in majority *Aurantivirga*, found abundant in enriched waters near red algae cultivation [85], and identified in algal blooms involved in algal polysaccharides degradation [86]. The core microbiota also contained *Nereida*, which could interact with its neighboring cells through quorum sensing and virulence factors [87]. Overall, the core microbiota in *Ulva lacunculata*'s cultures may be involved in providing metabolites for the algal host and protect it in the biofilm, and likely benefit from *Ulva*'s culture conditions in the water.

Due to their ability to uptake large concentrations of nitrate, *Ulva* are used as a biofilter of nitrogen loadings such as fish effluents in IMTA systems [33,34]. Indeed, nitrate-rich seawater enhances nitrate reductase activity in the non-axenic thallus from cultivated *Ulva fasciata* [88]. Moreover, nitrogen uptake is not only done by the cultivated algae but also by the associated microbial community [89,90]. As our experiment

allowed comparing *Ulva*'s bacterial community with and without nitrate fertilization, we investigated the three nitrate reduction pathways. The denitrification and DNRA pathways occur predominantly under anaerobic conditions in bacteria that use nitrate as an electron acceptor for respiration [91–93], whereas the ANRA pathway is activated under aerobic conditions to fuel cell growth [94,95]. Activation of the DNRA or denitrification pathways is regulated by the balance between carbon and nitrate concentrations (C/N ratio). A high C/N ratio stimulates the DNRA pathway, which produces ammonium and promotes biomass production, conserving bioavailable nitrogen in the culture ecosystem. Conversely, a low C/N ratio activates the denitrification pathway which produces unreactive dinitrogen gas which acts as a nitrogen sink [96–98]. In addition to being used as an alternative form of respiration when oxygen levels are low, denitrification can eliminate a surplus of reducing power (redox balance) or mitigate the toxicity of some nitrous oxide intermediates.

Nitrate fertilization of the *Ulva lacunculata*'s cultures had a major impact on the C/N balance. In the biofilm, nitrate reductase genes involved in the DNRA and denitrification pathways appeared to be more abundant in SW, whereas the dissimilatory nitrite reductase genes showed no systematic overabundance in either SW or ENR. In contrast, bacterial taxa carrying genes involved in denitrification were constantly overrepresented in ENR, suggesting an increased presence of bacteria able to dissipate excess inorganic nitrogen compounds from fertilization. These bacteria could divert an unknown proportion of the fertilizer transformed into gaseous N₂ but not involved in biomass growth. The large abundance of bacteria associated with the two pathways likely suggests anaerobic or microaerophilic conditions in the biofilm at the alga's surface, as previously hypothesized in the context of coastal *Ulva* blooms during night time and decomposition and as observed in similar marine ecological niches [99–101]. The effect of fertilization was noticeably different in the water. Reactions participating in all three nitrate reduction pathways consistently showed positive PBI, indicating a higher proportion of bacteria encoding the relevant enzymes in ENR. This suggests a shift in microbial communities towards enhanced nitrogen processing, as observed in aquatic bacterial communities near fish farms [102]. Noticeably, genes involved in the ANRA pathway were overrepresented in ENR and suggest biomass growth. Our results suggest that the response of the bacterial community to fertilization in terms of potential metabolic capacity is likely involved in producing gaseous nitrogen in the biofilm while biomass production may happen in the water.

Apart from the ubiquitous presence of *Glaciecola*, taxonomic composition of ASV involved in nitrate reduction differed between the two compartments, for SW and ENR. *Glaciecola* is known to be enhanced in *Ulva* culture conditions or green tide events [65,103], and can be a nitrate reducer producing dinitrogen [104]. In the biofilm, *Jannaschia* was also a dominant ASV associated with nitrate reduction metabolism in the two conditions. It may harbor the *nirB* (DNRA pathway) and *nasA* gene (ANRA) [105]. *Agaribacterium* was only found in the SW biofilm and may be able to reduce nitrate [106]. The ENR biofilm contained other dominant genera associated with nitrate reduction metabolism: *Roseobacter*, *Croceitalea*, and *Maribacter*. *Roseobacter* may be involved in reactions of the three pathways, as comparative genomics indicated that 6 out of 9 *Roseobacter* genomes included one or more of the following genes: *nasA*, *nirB*, *narG* and *nirK* [105]. *Maribacter* may reduce nitrate as observed in several strains [107], while *Croceitalea* may not be able to as seen in described strains [108–110]. In the SW water, *Ponticoccus* was dominant and it could be involved in nitrate reduction [111]. Amongst most abundant nitrate metabolizing genera in the ENR water, there were *Jannaschia* and *Roseobacter* like in the biofilm, but also *Marivita*, which may be able to reduce nitrate to nitrite [112]. The genera identified as involved in nitrate reduction metabolism may cooperate together to convert nitrate into ammonia or dinitrogen within the biofilm or aquatic environment.

4.4. Conclusion and perspectives

Our results highlight the influence of *Ulva lacinulata*'s cultivation and nitrate-based synthetic fertilizers in modulating the associated bacterial community in the biofilm and in the water. The bacterial community from the water was more reactive to nitrate supplementation than in the biofilm, implying a more stable community in this compartment. Noticeably, the core microbiota in the biofilm was likely involved in host fitness and physiology, raising the question of the potential microbial gardening by the host. Finally, our results in intensive cultivation conditions may be paralleled to what happens in nature in eutrophication conditions such as what has been observed with green tide events.

Our analyses also gave insights on the potential activity of the bacterial community in nitrate reduction and suggested metabolisms happening in anaerobic or microaerophilic conditions, that could happen during night time or decomposition events. Further experiments measuring the oxygen content in the biofilm, using microsensors for instance, and analyses on gene activity, such as with metatranscriptomics, may allow a more complete comprehension of the cultivated *Ulva* holobiont.

We focused on one component of the *Ulva* holobiont but a holistic approach including the other components should lead to a better understanding of the whole system in nitrate fertilization conditions. Indeed, the *Ulva* host [113,114] or other microbial groups, such as diatoms and microfungi [115–117] may be involved in nitrate reduction. A holistic approach may also include the physiology of the host and measurements of nitrogen accumulation in the host tissues, as the nitrogen metabolism of *Ulva* may influence the composition and functioning of its associated microbiota.

CRedit authorship contribution statement

Paul Estoup: Writing – original draft, Visualization, Software, Investigation, Formal analysis. **Vincent Gernigon:** Writing – review & editing, Investigation. **Amandine Avouac:** Writing – review & editing, Investigation. **Guillaume Blanc:** Writing – original draft, Validation, Supervision, Resources, Investigation, Funding acquisition, Conceptualization. **Angélique Gobet:** Writing – original draft, Validation, Supervision, Resources, Investigation, Funding acquisition, Conceptualization.

Declaration of competing interest

The authors have no conflict of interest to declare.

Data availability

Raw 16S rDNA sequences and sample metadata are available in the SRA under BioProject ID PRJNA1081356. The *rbcl* gene sequence is registered under the GenBank Accession number: PQ182749.

Acknowledgements

The authors warmly thank Patrick Raimbaud for nutrient analyses, Thibault Geoffroy for help retrieving samples, Ariane Atteia and Patricia Bonin for helpful discussions and Christine Felix, Florence Cornette, Jean-Luc Rolland, Uliana Podgourskaia, Fabrice Armougom and Sonia Bouchard for their technical support. A.G. acknowledges support from the Institut Français de Recherche pour l'Exploitation de la Mer (IFREMER), G.B. and A.A. acknowledge support from the Centre National de la Recherche Scientifique (CNRS). P.E. acknowledges support from Aix-Marseille Université (AMU). This work was supported by the Région Sud, the Institut Microbiologie, Bioénergies, et Biotechnologie (IM2B), and the IFREMER.

Appendix A. Supplementary data

Supplementary data to this article can be found online at <https://doi.org/10.1016/j.algal.2024.103688>.

References

- [1] A. Ménesguen, Les "marées vertes" en Bretagne, la responsabilité du nitrate, IFREMER/Centre de Brest, Direction de l'Environnement et de l'Aménagement du Littoral, Département d'Ecologie Côtière, B.P. 70, 29280 Plouzané, 2003.
- [2] V. Smetacek, A. Zingone, Green and golden seaweed tides on the rise, *Nature* 504 (2013) 84–88, <https://doi.org/10.1038/nature12860>.
- [3] I. Valiela, J. McClelland, J. Hauxwell, P.J. Behr, D. Hersh, K. Foreman, Macroalgal blooms in shallow estuaries: controls and ecophysiological and ecosystem consequences, *Limnol. Oceanogr.* 42 (1997) 1105–1118, https://doi.org/10.4319/lo.1997.42.5.part_2.1105.
- [4] Y. Feng, Y. Xiong, J.M. Hall-Spencer, K. Liu, J. Beardall, K. Gao, J. Ge, J. Xu, G. Gao, Shift in algal blooms from micro- to macroalgae around China with increasing eutrophication and climate change, *Glob. Change Biol.* 30 (2024) e17018, <https://doi.org/10.1111/gcb.17018>.
- [5] G. Gao, A.S. Clare, C. Rose, G.S. Caldwell, Eutrophication and warming-driven green tides (*Ulva rigida*) are predicted to increase under future climate change scenarios, *Mar. Pollut. Bull.* 114 (2017) 439–447, <https://doi.org/10.1016/j.marpolbul.2016.10.003>.
- [6] R.H. Charlier, P. Morand, C.W. Finkl, A. Thys, Green tides on the Brittany coasts, in: 2006 IEEE UESTU Balt. Int. Symp., IEEE, Klaipėda, Lithuania, 2006, pp. 1–13, <https://doi.org/10.1109/BALTIC.2006.7266128>.
- [7] M.-L. de Casabianca, N. Barthelemy, O. Serrano, A. Sfriso, Growth rate of *Ulva rigida* in different Mediterranean eutrophicated sites, *Bioresour. Technol.* 82 (2002) 27–31, [https://doi.org/10.1016/S0960-8524\(01\)00155-9](https://doi.org/10.1016/S0960-8524(01)00155-9).
- [8] D. Liu, J.K. Keesing, P. He, Z. Wang, Y. Shi, Y. Wang, The world's largest macroalgal bloom in the Yellow Sea, China: formation and implications, *Estuar. Coast. Shelf Sci.* 129 (2013) 2–10, <https://doi.org/10.1016/j.ecss.2013.05.021>.
- [9] R. Taylor, R.L. Fletcher, J.A. Raven, Preliminary studies on the growth of selected 'green tide' algae in laboratory culture: effects of irradiance, temperature, salinity and nutrients on growth rate, *Bot. Mar.* 44 (2001) 327–336, <https://doi.org/10.1515/BOT.2001.042>.
- [10] M.-L. de Casabianca, F. Posada, Effect of environmental parameters on the growth of *Ulva rigida* (Thau lagoon, France), *Bot. Mar.* 41 (1998) 157–166, <https://doi.org/10.1515/botm.1998.41.1-6.157>.
- [11] I. Valiela, G. Collins, J. Kremer, K. Lajtha, M. Geist, B. Seely, J. Brawley, C. H. Sham, Nitrogen loading from coastal watersheds to receiving estuaries: new method and application, *Ecol. Appl.* 7 (1997) 358–380, <https://doi.org/10.2307/2269505>.
- [12] B. Aa, L.B. Guldberg Lomstein, A.-T.A. Neubauer, J. Hansen, A. Donnelly, R. A. Herbert, P. Viaroli, G. Giordani, R. Azzoni, R. De Wit, K. Finster, Benthic decomposition of *Ulva lactuca*: a controlled laboratory experiment, *Aquat. Bot.* 85 (2006) 271–281, <https://doi.org/10.1016/j.aquabot.2006.05.006>.
- [13] R.I. Nedergaard, N. Risgaard-Petersen, K. Finster, The importance of sulfate reduction associated with *Ulva lactuca* thalli during decomposition: a mesocosm experiment, *J. Exp. Mar. Biol. Ecol.* 275 (2002) 15–29, [https://doi.org/10.1016/S0022-0981\(02\)00211-3](https://doi.org/10.1016/S0022-0981(02)00211-3).
- [14] M.C. Gauna, J.F. Escobar, M. Odorisio, E.J. Cáceres, E.R. Parodi, Spatial and temporal variation in algal epiphyte distribution on *Ulva* sp. (Ulvales, Chlorophyta) from northern Patagonia in Argentina, *Phycologia* 56 (2017) 125–135, <https://doi.org/10.2216/16-51.1>.
- [15] S. Loiseaux, Morphologie et cytologie des Myrionémacées, *Critères taxonomiques.*, *Rev. Générale Bot.* 74 (1967) 329–347.
- [16] S. Egan, T. Harder, C. Burke, P. Steinberg, S. Kjelleberg, T. Thomas, The seaweed holobiont: understanding seaweed–bacteria interactions, *FEMS Microbiol. Rev.* 37 (2013) 462–476, <https://doi.org/10.1111/1574-6976.12011>.
- [17] E. Armstrong, A. Rogerson, J.W. Leftley, The abundance of heterotrophic protists associated with intertidal seaweeds, *Estuar. Coast. Shelf Sci.* 50 (2000) 415–424, <https://doi.org/10.1006/ecss.1999.0577>.
- [18] M. Bengtsson, K. Sjøtun, L. Øvreås, Seasonal dynamics of bacterial biofilms on the kelp (*Laminaria hyperborea*), *Aquat. Microb. Ecol.* 60 (2010) 71–83, <https://doi.org/10.3354/ame01409>.
- [19] S. Egan, T. Thomas, S. Kjelleberg, Unlocking the diversity and biotechnological potential of marine surface associated microbial communities, *Curr. Opin. Microbiol.* 11 (2008) 219–225, <https://doi.org/10.1016/j.mib.2008.04.001>.
- [20] L. Provasoli, Effect of plant hormones on *Ulva*, *Biol. Bull.* 114 (1958) 375–384, <https://doi.org/10.2307/1538992>.
- [21] T. Thomas, F.F. Evans, D. Schleheck, A. Mai-Prochnow, C. Burke, A. Penesyan, D. S. Dalisay, S. Stelzer-Braid, N. Saunders, J. Johnson, S. Ferreira, S. Kjelleberg, S. Egan, Analysis of the *Pseudoalteromonas tunicata* genome reveals properties of a surface-associated life style in the marine environment, *PLoS One* 3 (2008) e3252, <https://doi.org/10.1371/journal.pone.0003252>.
- [22] J. Hylleberg, Selective feeding by *Abarenicola pacifica* with notes on *Abarenicola vagabunda* and a concept of gardening in lugworms, *Ophelia* 14 (1975) 113–137, <https://doi.org/10.1080/00785236.1975.10421972>.
- [23] M. Saha, F. Weinberger, Microbial "gardening" by a seaweed holobiont: surface metabolites attract protective and deter pathogenic epibacterial settlement, *J. Ecol.* 107 (2019) 1365–2745, <https://doi.org/10.1111/1365-2745.13193>.

- [24] R.W. Kessler, A. Weiss, S. Kuegler, C. Hermes, T. Wichard, Macroalgal-bacterial interactions: role of dimethylsulfoniopropionate in microbial gardening by *Ulva* (Chlorophyta), *Mol. Ecol.* 27 (2018) 1808–1819, <https://doi.org/10.1111/mec.14472>.
- [25] S. Egan, N.D. Fernandes, V. Kumar, M. Gardiner, T. Thomas, Bacterial pathogens, virulence mechanism and host defence in marine macroalgae, *Environ. Microbiol.* 16 (2014) 925–938, <https://doi.org/10.1111/1462-2920.12288>.
- [26] S. Egan, M. Gardiner, Microbial dysbiosis: rethinking disease in marine ecosystems, *Front. Microbiol.* 7 (2016) 991, <https://doi.org/10.3389/fmicb.2016.00991>.
- [27] L. Provasoli, L.J. Pintner, Bacteria induced polymorphism in an axenic laboratory strain of *Ulva Lactuca* (Chlorophyceae)¹, *J. Phycol.* 16 (1980) 196–201, <https://doi.org/10.1111/j.1529-8817.1980.tb03019.x>.
- [28] F. Ghaderiardakani, J.C. Coates, T. Wichard, Bacteria-induced morphogenesis of *Ulva intestinalis* and *Ulva mutabilis* (Chlorophyta): a contribution to the lottery theory, *FEMS Microbiol. Ecol.* 93 (2017) fix094, <https://doi.org/10.1093/femsec/fix094>.
- [29] M. Spoerner, T. Wichard, T. Bachhuber, J. Stratmann, W. Oertel, Growth and thallus morphogenesis of *Ulva mutabilis* (Chlorophyta) depends on a combination of two bacterial species excreting regulatory factors, *J. Phycol.* 48 (2012) 1433–1447, <https://doi.org/10.1111/j.1529-8817.2012.01231.x>.
- [30] P. Wienecke, J.F. Ulrich, C.F. Morales-Reyes, S. Dhiman, T. Wichard, H. Arndt, Enantio-selective Total Synthesis of the Morphogen (–)-Thalussin and Mediated Uptake of Fe(III) into the Green Seaweed *Ulva*, *Chem. – Eur. J.* 30 (2024) e202304007, <https://doi.org/10.1002/chem.202304007>.
- [31] F. Ghaderiardakani, G. Califano, J. Mohr, M. Abreu, J. Coates, T. Wichard, Analysis of algal growth- and morphogenesis- promoting factors in an integrated multi-trophic aquaculture system for farming *Ulva* spp, *Aquac. Environ. Interact.* 11 (2019) 375–391, <https://doi.org/10.3354/aei00319>.
- [32] J. Hardegen, G. Amend, T. Wichard, Lifecycle-dependent toxicity and removal of micropollutants in algal cultures of the green seaweed *Ulva* (Chlorophyta), *J. Appl. Phycol.* 35 (2023) 2031–2048, <https://doi.org/10.1007/s10811-023-02936-x>.
- [33] L. Guttman, S.E. Boxman, R. Barkan, A. Neori, M. Shpigel, Combinations of *Ulva* and periphyton as biofilters for both ammonia and nitrate in mariculture fishpond effluents, *Algal Res.* 34 (2018) 235–243, <https://doi.org/10.1016/j.algal.2018.08.002>.
- [34] A. Neori, F.E. Msuya, L. Shauli, A. Schuenhoff, F. Kopel, M. Shpigel, A novel three-stage seaweed (*Ulva lactuca*) biofilter design for integrated mariculture, *J. Appl. Phycol.* 15 (2003) 543–553, <https://doi.org/10.1023/B:JAPH.000004382.89142.2d>.
- [35] D. Nguyen, O. Ovadia, L. Guttman, Temporal force governs the microbial assembly associated with *Ulva fasciata* (Chlorophyta) from an integrated multi-trophic aqua-culture system, *Front. Microbiol.* 14 (2023) 1223204, <https://doi.org/10.3389/fmicb.2023.1223204>.
- [36] E. Metaxa, G. Deviller, P. Pagand, C. Alliaume, C. Casellas, J.P. Blancheton, High rate algal pond treatment for water reuse in a marine fish recirculation system: water purification and fish health, *Aquaculture* 252 (2006) 92–101, <https://doi.org/10.1016/j.aqua-culture.2005.11.053>.
- [37] B. Barrut, J.-P. Blancheton, A. Muller-Feuga, F. René, C. Narváez, J.-Y. Champagne, A. Grasmick, Separation efficiency of a vacuum gas lift for microalgae harvesting, *Bioresour. Technol.* 128 (2013) 235–240, <https://doi.org/10.1016/j.biortech.2012.10.056>.
- [38] F. Thomas, T. Barbeyron, G. Michel, Evaluation of reference genes for real-time quantitative PCR in the marine flavobacterium *Zobellia galactanivorans*, *J. Microbiol. Methods* 84 (2011) 61–66, <https://doi.org/10.1016/j.mimet.2010.10.016>.
- [39] A. Aminot, R. Kérouel, Hydrologie des écosystèmes marins: paramètres et analyses, Ifremer; Diffusion, INRA éditions, Versailles, Plouzané, 2004.
- [40] A. Aminot, R. Kérouel, Dosage automatique des nutriments dans les eaux marines: méthodes en flux continu, Ifremer, France, 2007.
- [41] R.M. Holmes, A. Aminot, R. Kérouel, B.A. Hooker, B.J. Peterson, A simple and precise method for measuring ammonium in marine and freshwater ecosystems, *Can. J. Fish. Aquat. Sci.* 56 (1999) 1801–1808, <https://doi.org/10.1139/f99-128>.
- [42] B.W. Taylor, C.F. Keep, R.O. Hall, B.J. Koch, L.M. Tronstad, A.S. Flecker, A. J. Ulseth, Improving the fluorometric ammonium method: matrix effects, background fluorescence, and standard additions, *J. North Am. Benthol. Soc.* 26 (2007) 167–177, [https://doi.org/10.1899/0887-3593\(2007\)26\[167:ITFAMM\]2.0.CO;2](https://doi.org/10.1899/0887-3593(2007)26[167:ITFAMM]2.0.CO;2).
- [43] P. Raimbault, F. Lantoine, J. Neveux, Dosage rapide de la chlorophylle a et des phéopigments a par fluorimétrie après extraction au méthanol. Comparaison avec la méthode classique d'extraction à l'acétone., *Océan, Sér. Doc. Océan.* 30 (2004) 189–205.
- [44] M. Martin, Cutadapt removes adapter sequences from high-throughput sequencing reads, *EMBnet.J.* 17 (2011) 10–12, <https://doi.org/10.14806/ej.17.1.200>.
- [45] B.J. Callahan, P.J. McMurdie, M.J. Rosen, A.W. Han, A.J.A. Johnson, S.P. Holmes, DADA2: high-resolution sample inference from Illumina amplicon data, *Nat. Methods* 13 (2016) 581–583, <https://doi.org/10.1038/nmeth.3869>.
- [46] R Core Team, R: A Language and Environment for Statistical Computing. <https://www.R-project.org/>, 2022.
- [47] C. Quast, E. Pruesse, P. Yilmaz, J. Gerken, T. Schweer, P. Yarza, J. Peplies, F. O. Glöckner, The SILVA ribosomal RNA gene database project: improved data processing and web-based tools, *Nucleic Acids Res.* 41 (2012) D590–D596, <https://doi.org/10.1093/nar/gks1219>.
- [48] P. Yilmaz, L.W. Parfrey, P. Yarza, J. Gerken, E. Pruesse, C. Quast, T. Schweer, J. Peplies, W. Ludwig, F.O. Glöckner, The SILVA and “all-species living tree project (LTP)” taxo-nomic frameworks, *Nucleic Acids Res.* 42 (2014) D643–D648, <https://doi.org/10.1093/nar/gkt1209>.
- [49] L. Lahti, S. Shetty, *Microbiome R Package*, 2012.
- [50] D.H. Ogle, J.C. Doll, A.P. Wheeler, A. Dinno, FSA: Simple Fisheries Stock Assessment Methods. <https://CRAN.R-project.org/package=FSA>, 2023.
- [51] J. Palarea-Albaladejo, J.A. Martín-Fernández, Compositions — R package for multivariate imputation of left-censored data under a compositional approach, *Chemom. Intel. Lab. Syst.* 143 (2015) 85–96, <https://doi.org/10.1016/j.chemolab.2015.02.019>.
- [52] G.B. Gloor, J.M. Macklaim, V. Pawlowsky-Glahn, J.J. Egozcue, Microbiome datasets are compositional: and this is not optional, *Front. Microbiol.* 8 (2017) 2224, <https://doi.org/10.3389/fmicb.2017.02224>.
- [53] J. Aitchison, The statistical analysis of compositional data, *J. R. Stat. Soc.* 44 (1986) 139–160.
- [54] P.J. McMurdie, S. Holmes, phyloseq: an R package for reproducible interactive analysis and graphics of microbiome census data, *PLoS One* 8 (2013) e61217, <https://doi.org/10.1371/journal.pone.0061217>.
- [55] J. Oksanen, G. Simpson, F. Blanchet, R. Kindt, P. Legendre, P. Minchin, R. O'Hara, P. Solymos, M. Stevens, E. Szoecs, H. Wagner, M. Barbour, M. Bedward, B. Bolker, D. Borcard, G. Carvalho, M. Chirico, M. De Caceres, S. Durand, H. Evangelista, R. FitzJohn, M. Friendly, B. Furneaux, G. Hannigan, M. Hill, L. Lahti, D. McGlenn, M. Ouellette, E. Ribeiro Cunha, T. Smith, A. Stier, C. Ter Braak, J. Weedon, Vegan: Community Ecology Package. <https://CRAN.R-project.org/package=vegan>, 2022.
- [56] D. Borcard, P. Legendre, P. Drapeau, Partialling out the spatial component of ecological variation, *Ecology* 73 (1992) 1045–1055, <https://doi.org/10.2307/1940179>.
- [57] G.M. Douglas, V.J. Maffei, J.R. Zaneveld, S.N. Yurgel, J.R. Brown, C.M. Taylor, C. Huttenhower, M.G.I. Langille, PICRUSt2 for prediction of metagenome functions, *Nat. Biotechnol.* 38 (2020) 685–688, <https://doi.org/10.1038/s41587-020-0548-x>.
- [58] V.M. Markowitz, I.-M.A. Chen, K. Palaniappan, K. Chu, E. Szeto, Y. Grechkin, A. Ratner, B. Jacob, J. Huang, P. Williams, M. Huntemann, I. Anderson, K. Mavromatis, N.N. Ivanova, N.C. Kyrpides, IMG: the integrated microbial genomes database and comparative analysis system, *Nucleic Acids Res.* 40 (2012), <https://doi.org/10.1093/nar/gkr1044>, D115–D122.
- [59] M. Kanehisa, Toward understanding the origin and evolution of cellular organisms, *Protein Sci. Publ. Protein Soc.* 28 (2019) 1947–1951, <https://doi.org/10.1002/pro.3715>.
- [60] M. Kanehisa, M. Furumichi, Y. Sato, M. Kawashima, M. Ishiguro-Watanabe, KEGG for taxonomy-based analysis of pathways and genomes, *Nucleic Acids Res.* 51 (2023) D587–D592, <https://doi.org/10.1093/nar/gkac963>.
- [61] M. Kanehisa, S. Goto, KEGG: Kyoto Encyclopedia of Genes and Genomes, *Nucleic Acids Res.* 28 (2000) 27–30, <https://doi.org/10.1093/nar/28.1.27>.
- [62] C. Burke, T. Thomas, M. Lewis, P. Steinberg, S. Kjelleberg, Composition, uniqueness and variability of the epiphytic bacterial community of the green alga *Ulva australis*, *ISME J.* 5 (2011) 590–600, <https://doi.org/10.1038/ismej.2010.164>.
- [63] N.B. Comba González, A.N. Niño Corredor, L. López Kleine, D. Montoya Castaño, Temporal changes of the epiphytic bacteria community from the marine macroalga *Ulva lactuca* (Santa Marta, Colombian-Caribbean), *Curr. Microbiol.* 78 (2021) 534–543, <https://doi.org/10.1007/s00284-020-02302-x>.
- [64] L.M. van der Loos, S. D'hondt, A.H. Engelen, H. Pavia, G.B. Toth, A. Willems, F. Weinberger, O. De Clerck, S. Steinhagen, Salinity and host drive *Ulva*-associated bacterial communities across the Atlantic–Baltic Sea gradient, *Mol. Ecol.* 32 (2022) 6260–6277, <https://doi.org/10.1111/mec.16462>.
- [65] G. Califano, M. Kwantes, M.H. Abreu, R. Costa, T. Wichard, Cultivating the macroalgal holobiont: effects of integrated multi-trophic aquaculture on the microbiome of *Ulva rigida* (Chlorophyta), *Front. Mar. Sci.* 7 (2020) 52, <https://doi.org/10.3389/fmars.2020.00052>.
- [66] I.H. Tan, J. Blomster, G. Hansen, E. Leskinen, C.A. Maggs, D.G. Mann, H. J. Sluiman, M.J. Stanhope, Molecular phylogenetic evidence for a reversible morphogenetic switch controlling the gross morphology of two common genera of green seaweeds, *Ulva* and *Enteromorpha*, *Mol. Biol. Evol.* 16 (1999) 1011–1018, <https://doi.org/10.1093/oxfordjournals.molbev.a026190>.
- [67] H.S. Hayden, J. Blomster, C.A. Maggs, P.C. Silva, M.J. Stanhope, J.R. Waaland, Linnaeus was right all along: *Ulva* and *Enteromorpha* are not distinct genera, *Eur. J. Phycol.* 38 (2003) 277–294, <https://doi.org/10.1080/1364253031000136321>.
- [68] M.B. Batista, R.L. Cunha, R. Castilho, P.A. Horta, Sea lettuce systematics: lumping or splitting, *bioRxiv* (2018) 413450, <https://doi.org/10.1101/413450>.
- [69] S. Steinhagen, R. Karez, F. Weinberger, Cryptic, alien and lost species: molecular diversity of *Ulva sensu lato* along the German coasts of the North and Baltic Seas, *Eur. J. Phycol.* 54 (2019) 466–483, <https://doi.org/10.1080/09670262.2019.1597925>.
- [70] J.R. Hughey, P.W. Gabrielson, C.A. Maggs, F. Mineur, Genomic analysis of the lectotype specimens of European *Ulva rigida* and *Ulva lacunculata* (Ulvaceae, Chlorophyta) reveals the ongoing misapplication of names, *Eur. J. Phycol.* 57 (2021) 143–153, <https://doi.org/10.1080/09670262.2021.1914862>.
- [71] S. Steinhagen, S. Hoffmann, H. Pavia, G.B. Toth, Molecular identification of the ubiquitous green algae *Ulva* reveals high biodiversity, crypticity, and invasive species in the Atlantic-Baltic Sea region, *Algal Res.* 103132 (2023), <https://doi.org/10.1016/j.algal.2023.103132>.

- [72] J. Hollants, F. Leliaert, O. De Clerck, A. Willems, What we can learn from sushi: a review on seaweed-bacterial associations, *FEMS Microbiol. Ecol.* 83 (2013) 1–16, <https://doi.org/10.1111/j.1574-6941.2012.01446.x>.
- [73] L.M. van der Loos, S. D'hondt, A. Willems, O. De Clerck, Characterizing algal microbiomes using long-read nanopore sequencing, *Algal Res.* 59 (2021) 102456, <https://doi.org/10.1016/j.algal.2021.102456>.
- [74] A.J. Roth-Schulze, J. Pintado, E. Zozaya-Valdés, J. Cremades, P. Ruiz, S. Kjelleberg, T. Thomas, Functional biogeography and host specificity of bacterial communities associated with the marine green alga *Ulva* spp, *Mol. Ecol.* 27 (2018) 1952–1965, <https://doi.org/10.1111/mec.14529>.
- [75] K.L. Morrissey, L. Çavaş, A. Willems, O. De Clerck, Disentangling the influence of environment, host specificity and thallus differentiation on bacterial communities in siphonous green seaweeds, *Front. Microbiol.* 10 (2019) 717, <https://doi.org/10.3389/fmicb.2019.00717>.
- [76] K.L. Morrissey, L. Ivesa, S. Delva, S. D'Hondt, A. Willems, O. De Clerck, Impacts of environmental stress on resistance and resilience of algal-associated bacterial communities, *Ecol. Evol.* 11 (2021) 15004–15019, <https://doi.org/10.1002/ece3.8184>.
- [77] T. Staufenberger, V. Thiel, J. Wiese, J.F. Imhoff, Phylogenetic analysis of bacteria associated with *Laminaria saccharina*, *FEMS Microbiol. Ecol.* 64 (2008) 65–77, <https://doi.org/10.1111/j.1574-6941.2008.00445.x>.
- [78] J. Pinhassi, L. Gómez-Consarnau, L. Alonso-Sáez, M. Sala, M. Vidal, C. Pedrós-Alió, J. Gasol, Seasonal changes in bacterioplankton nutrient limitation and their effects on bacterial community composition in the NW Mediterranean Sea, *Aquat. Microb. Ecol.* 44 (2006) 241–252, <https://doi.org/10.3354/ame044241>.
- [79] H. Schäfer, L. Bernard, C. Courties, P. Lebaron, P. Servais, R. Pukall, E. Stackebrandt, M. Troussellier, T. Guindulain, J. Vives-Rego, G. Muyzer, Microbial community dynamics in Mediterranean nutrient-enriched seawater mesocosms: changes in the genetic diversity of bacterial populations, *FEMS Microbiol. Ecol.* 34 (2001) 243–253, <https://doi.org/10.1111/j.1574-6941.2001.tb00775.x>.
- [80] A. Shade, J. Handelsman, Beyond the Venn diagram: the hunt for a core microbiome, *Environ. Microbiol.* 14 (2012) 4–12, <https://doi.org/10.1111/j.1462-2920.2011.02585.x>.
- [81] A. Risely, Applying the core microbiome to understand host–microbe systems, *J. Anim. Ecol.* 89 (2020) 1549–1558, <https://doi.org/10.1111/1365-2656.13229>.
- [82] B.L. Weigel, K.K. Miranda, E.C. Fogarty, A.R. Watson, C.A. Pfister, Functional insights into the kelp microbiome from metagenome-assembled genomes, *mSystems* 7 (2022) e01422–21, <https://doi.org/10.1128/mSystems.01422-21>.
- [83] T. Wichard, Exploring bacteria-induced growth and morphogenesis in the green macroalga order Ulvales (Chlorophyta), *Front. Plant Sci.* 6 (2015) 86, <https://doi.org/10.3389/fpls.2015.00086>.
- [84] D. Rao, J.S. Webb, C. Holmström, R. Case, A. Low, P. Steinberg, S. Kjelleberg, Low densities of epiphytic bacteria from the marine alga *Ulva australis* inhibit settlement of fouling organisms, *Appl. Environ. Microbiol.* 73 (2007) 7844–7852, <https://doi.org/10.1128/AEM.01543-07>.
- [85] N. Xu, W. Wang, K. Xu, Y. Xu, D. Ji, C. Chen, C. Xie, Cultivation of different seaweed species and seasonal changes cause divergence of the microbial community in coastal seawaters, *Front. Microbiol.* 13 (2022) 988743.
- [86] K. Krüger, M. Chafee, T. Ben Francis, T. Glavina del Rio, D. Becher, T. Schweder, R.L. Amann, H. Teeling, In marine *Bacteroidetes* the bulk of glycan degradation during algae blooms is mediated by few clades using a restricted set of genes, *ISME J.* 13 (2019) 2800–2816, <https://doi.org/10.1038/s41396-019-0476-y>.
- [87] D.R. Arahal, M.J. Pujalte, L. Rodrigo-Torres, Draft genomic sequence of *Nereida ignava* CECT 5292^T, a marine bacterium of the family *Rhodobacteraceae*, *Stand Genomic Sci.* 11 (2016) 1–8, <https://doi.org/10.1186/s40793-016-0141-2>.
- [88] B. Shahar, M. Shpigel, R. Barkan, M. Masasa, A. Neori, H. Chernov, E. Salomon, M. Kiflawi, L. Guttman, Changes in metabolism, growth and nutrient uptake of *Ulva fasciata* (Chlorophyta) in response to nitrogen source, *Algal Res.* 46 (2020) 101781, <https://doi.org/10.1016/j.algal.2019.101781>.
- [89] T. Ben Ari, A. Neori, D. Ben-Ezra, L. Shauli, V. Odintsov, M. Shpigel, Management of *Ulva lactuca* as a biofilter of mariculture effluents in IMTA system, *Aquaculture* 434 (2014) 493–498, <https://doi.org/10.1016/j.aquaculture.2014.08.034>.
- [90] R. Crab, Y. Avnimelech, T. Defoirdt, P. Bossier, W. Verstraete, Nitrogen removal techniques in aquaculture for a sustainable production, *Aquaculture* 270 (2007) 1–14, <https://doi.org/10.1016/j.aquaculture.2007.05.006>.
- [91] B. Kraft, H.E. Tegetmeyer, R. Sharma, M.G. Klotz, T.G. Ferdelman, R.L. Hettich, J. S. Geelhoed, M. Strous, The environmental controls that govern the end product of bacterial nitrate respiration, *Science* 345 (2014) 676–679, <https://doi.org/10.1126/science.1254070>.
- [92] L. Philippot, S. Hallin, M. Schlöter, Ecology of Denitrifying Prokaryotes in Agricultural Soil, in: *Adv. Academic Press, Agron.*, 2007, pp. 249–305, [https://doi.org/10.1016/S0065-2113\(07\)96003-4](https://doi.org/10.1016/S0065-2113(07)96003-4).
- [93] J. Tiedje, Ecology of denitrification and dissimilatory nitrate reduction to ammonium, in: *Methods Soil Anal. Part 2 Chem. Microbiol. Prop., Biology of Anaerobic Micro-organisms*, 1988, pp. 179–244.
- [94] P. Cabello, M.D. Roldán, F. Castillo, C. Moreno-Vivián, Nitrogen cycle, in: *Encycl. Microbiol.*, Elsevier, 2009, pp. 299–321, <https://doi.org/10.1016/B978-012373944-5.00055-9>.
- [95] Y. Li, Y. Wang, L. Fu, Y. Gao, H. Zhao, W. Zhou, Aerobic-heterotrophic nitrogen removal through nitrate reduction and ammonium assimilation by marine bacterium *Vibrio* sp. Y1-5, *Bioresour. Technol.* 230 (2017) 103–111, <https://doi.org/10.1016/j.biortech.2017.01.049>.
- [96] A. Pandey, H. Suter, J.-Z. He, H.-W. Hu, D. Chen, Dissimilatory nitrate reduction to ammonium dominates nitrate reduction in long-term low nitrogen fertilized rice paddies, *Soil Biol. Biochem.* 131 (2019) 149–156, <https://doi.org/10.1016/j.soilbio.2019.01.007>.
- [97] S.X. Yin, D. Chen, L.M. Chen, R. Edis, Dissimilatory nitrate reduction to ammonium and responsible microorganisms in two Chinese and Australian paddy soils, *Soil Biol. Biochem.* 34 (2002) 1131–1137, [https://doi.org/10.1016/S0038-0717\(02\)00049-4](https://doi.org/10.1016/S0038-0717(02)00049-4).
- [98] S. Yoon, C. Cruz-García, R. Sanford, K.M. Ritalahti, F.E. Löffler, Denitrification versus respiratory ammonification: environmental controls of two competing dissimilatory NO₃/NO₂ reduction pathways in *Shewanella loihica* strain PV-4, *ISME J.* 9 (2015) 1093–1104, <https://doi.org/10.1038/ismej.2014.201>.
- [99] V. Michotey, P. Bonin, Evidence for anaerobic bacterial processes in the water column: denitrification and dissimilatory nitrate ammonification in the northwestern Mediterranean Sea, *Mar. Ecol. Prog. Ser.* 160 (1997) 47–56.
- [100] A. Schramm, D. De Beer, A. Gieseke, R. Amann, Microenvironments and distribution of nitrifying bacteria in a membrane-bound biofilm, *Environ. Microbiol.* 2 (2000) 680–686, <https://doi.org/10.1046/j.1462-2920.2000.00150.x>.
- [101] X. Zhang, Y. Song, D. Liu, J.K. Keesing, J. Gong, Macroalgal blooms favor heterotrophic diazotrophic bacteria in nitrogen-rich and phosphorus-limited coastal surface waters in the Yellow Sea, *Estuar. Coast. Shelf Sci.* 163 (2015) 75–81, <https://doi.org/10.1016/j.ecss.2014.12.015>.
- [102] L.S.H. Lo, Z. Xu, S.S. Lee, W.K. Lau, J.-W. Qiu, H. Liu, P.-Y. Qian, J. Cheng, How elevated nitrogen load affects bacterial community structure and nitrogen cycling services in coastal water, *Front. Microbiol.* 13 (2022) 1062029, <https://doi.org/10.3389/fmicb.2022.1062029>.
- [103] X. Wang, H. Yu, Y. Li, Q. Fu, H. Shao, H. He, M. Wang, Metatranscriptomic insights into the microbial metabolic activities during an *Ulva prolifera* green tide in coastal Qingdao areas, *Environ. Pollut.* 343 (2024) 123217, <https://doi.org/10.1016/j.envpol.2023.123217>.
- [104] L.-P. Chen, H.-Y. Xu, S.-Z. Fu, H.-X. Fan, Y.-H. Liu, S.-J. Liu, Z.-P. Liu, *Glaciecola lipolytica* sp. nov., isolated from seawater near Tianjin city, China, *Int. J. Syst. Evol. Microbiol.* 59 (2009) 73–76, <https://doi.org/10.1099/ijs.0.000489-0>.
- [105] H. Luo, M.A. Moran, Evolutionary ecology of the marine *Roseobacter* clade, *Microbiol. Mol. Biol. Rev.* 78 (2014) 573–587, <https://doi.org/10.1128/MMBR.00020-14>.
- [106] Z. Huang, Q. Lai, D. Zhang, Z. Shao, *Agaribacterium haliotis* gen. nov., sp. nov., isolated from abalone faeces, *Int. J. Syst. Evol. Microbiol.* 67 (2017) 3819–3823, <https://doi.org/10.1099/ijsem.0.002199>.
- [107] O.I. Nedashkovskaya, S.B. Kim, V.V. Mikhailov, *Maribacter stanieri* sp. nov., a marine bacterium of the family *Flavobacteriaceae*, *Int. J. Syst. Evol. Microbiol.* 60 (2010) 214–218, <https://doi.org/10.1099/ijs.0.012286-0>.
- [108] M. Kim, I.-T. Cha, H.W. Lee, K.J. Yim, H.S. Song, D.-W. Hyun, J.-W. Bae, S. W. Roh, S.-J. Lee, *Croceitalea litorea* sp. nov., isolated from seashore sand, *Int. J. Syst. Evol. Microbiol.* 65 (2015) 4563–4567, <https://doi.org/10.1099/ijsem.0.000613>.
- [109] H.-S. Lee, K.K. Kwon, S.-H. Yang, S.S. Bae, C.H. Park, S.-J. Kim, J.-H. Lee, Description of *Croceitalea* gen. nov. in the family *Flavobacteriaceae* with two species, *Croceitalea eckloniae* sp. nov. and *Croceitalea dokdonensis* sp. nov., isolated from the rhizosphere of the marine alga *Ecklonia kurome*, *Int. J. Syst. Evol. Microbiol.* 58 (2008) 2505–2510, <https://doi.org/10.1099/ijs.0.65697-0>.
- [110] Y. Su, M. Yu, Q. Ren, Z. Sun, Y. Zhang, X. Yang, Y. Wang, X.-H. Zhang, *Croceitalea marina* sp. nov., isolated from marine particles of Yellow Sea, and emended description of the genera *Croceitalea*, *Int. J. Syst. Evol. Microbiol.* 67 (2017) 4253–4259, <https://doi.org/10.1099/ijsem.0.002298>.
- [111] C.Y. Hwang, B.C. Cho, *Ponticoccus litoralis* gen. nov., sp. nov., a marine bacterium in the family *Rhodobacteraceae*, *Int. J. Syst. Evol. Microbiol.* 58 (2008) 1332–1338, <https://doi.org/10.1099/ijs.0.65612-0>.
- [112] J.-H. Yoon, S.-J. Kang, J.-S. Lee, *Marivita geojedonensis* sp. nov., isolated from seawater, *Int. J. Syst. Evol. Microbiol.* 63 (2013) 423–427, <https://doi.org/10.1099/ijs.0.039065-0>.
- [113] X. Fan, D. Xu, D. Wang, Y. Wang, X. Zhang, N. Ye, Nutrient uptake and transporter gene expression of ammonium, nitrate, and phosphorus in *Ulva linza*: adaption to variable concentrations and temperatures, *J. Appl. Phycol.* 32 (2020) 1311–1322, <https://doi.org/10.1007/s10811-020-02050-2>.
- [114] A. Ménesguen, J.-Y. Piriou, Nitrogen loadings and macroalgal (*Ulva* sp.) mass accumulation in Brittany (France), *Ophelia* 42 (1995) 227–237, <https://doi.org/10.1080/00785326.1995.10431506>.
- [115] A. Kamp, D. de Beer, J.L. Nitsch, G. Lavik, P. Stief, Diatoms respire nitrate to survive dark and anoxic conditions, *Proc. Natl. Acad. Sci.* 108 (2011) 5649–5654, <https://doi.org/10.1073/pnas.1015744108>.
- [116] A. Kamp, S. Høgslund, N. Risgaard-Petersen, P. Stief, Nitrate storage and dissimilatory nitrate reduction by eukaryotic microbes, *Front. Microbiol.* 6 (2015) 1492, <https://doi.org/10.3389/fmicb.2015.01492>.
- [117] C.S. Manohar, L.D. Menezes, K.P. Ramasamy, R.M. Meena, Phylogenetic analyses and nitrate-reducing activity of fungal cultures isolated from the permanent, oceanic oxygen minimum zone of the Arabian Sea, *Can. J. Microbiol.* 61 (2015) 217–226, <https://doi.org/10.1139/cjm-2014-0507>.